

REUSING STONES IN MEDIEVAL CHURCHES: A MULTIDISCIPLINARY APPROACH TO SAN MARTIÑO DE ARMENTAL (NW SPAIN)

José Carlos Sánchez-Pardo

Department of History, University of Santiago de Compostela (Spain)

<https://orcid.org/0000-0003-2899-4951>

josecarlos.sanchez@usc.es

Telephone: (+34)881811000 ext. 12561

Rebeca Blanco-Rotea

Department of History, University of Santiago de Compostela (Spain); Visiting
Research Fellow at Unit of Archaeology, University of Minho (Portugal)

<https://orcid.org/0000-0003-3975-2149>

Jorge Sanjurjo-Sánchez

University Institute of Geology – CULXEO research group, University of A Coruña, A
Coruña (Spain)

<https://orcid.org/0000-0002-7559-8647>

Victor Barrientos-Rodríguez

Department of Civil Engineering – CULXEO research group, University of A Coruña
(Spain)

<https://orcid.org/0000-0002-8004-2790>

Acknowledgements

This study has been carried out as a part of the projects titled: “EMCHAHE” funded by a Marie Curie Career Integration Grant from the European Union as well as “Consiliencia II” and “TERPOMED”, funded by Galician Regional Government. We would like to thank the following people who collaborated on the project: Patricia Mañana (CSIC), for her help with the geometric documentation of the buildings that were studied; José Manuel Costa (USC) for his work on the site of Cidadela, and the prospecting work carried out in Armental; and Helena Gimeno (UAH) for her help with the epigraphs. We are also grateful to Professor Marco García-Quintela (USC) for his help in implementing the project in the USC. And finally, our thanks to the archdiocese of Santiago de Compostela for its help in studying this and other buildings, and to the neighbours of Armental for the information they provided, and their kind collaboration.

Abstract

This paper presents an interdisciplinary methodology to help better understand the evolution of the use and re-use of stone material in the construction sequence of historical buildings. A combination of petrological analyses, stratigraphic analyses of walls, geochemical characterisation and absolute dating of mortars using optically stimulated luminescence and radiocarbon dating, the study of written sources and photogrammetry, is applied to the case study of San Martiño de Armental, a rural parish church from NW Iberia. Results reveal a much more complex history and evolution than previously thought for this church, with the discovery of the remains of a 10th century AD building still

standing in some parts of the building. This first church was already made of reused ashlar from one or several unknown buildings. Later romanesque and modern phases still reuse some of these ashlar while incorporate new stone material. All the stones and mortars of the church seem to have local origin, although there are differences in their composition depending of the construction phase they belong to. Basing on these results, we will discuss in the last part of the paper how re-use of materials can become an interesting reflection of the different construction techniques used and the level of economic investment made by those who promoted the work.

Keywords

Optically Stimulated Luminescence, Petrology, Archaeology of Architecture, Medieval churches, Photogrammetry

1. INTRODUCTION

Presentation

The re-use of stone is something that can be found quite frequently in medieval churches throughout all of Europe, and which has been explored in a large number of studies from a historical, archaeological, and artistic perspective (i. e. Brenk 1987; Greenhalgh 1989; Quirós 1998; Ward-Perkins 1999; Cutler 1999; Eaton 2000; Araguas 2007; Domingo 2009; Utrero and Sastre 2012). However, the majority of these studies have focused on the most monumental and outstanding cases at historical and artistic level, about which there is more textual and archaeological information, overlooking a multitude of small, unassuming churches, especially in rural areas, even if they can also shed important light on their surrounding historical and archaeological territorial dynamics (Wood 2006; La Rocca 2007; Quirós and Fernández 2012; Sánchez-Pardo 2015). Furthermore, to date, it has been difficult to identify the source of the stone blocks, their original chronology, and the information they can provide us with on the building of which they form a part.

In this study, we present an interdisciplinary method to help better understand the evolution of the use and re-use of stone material in the construction history of an ancient building about which there is hardly any written information. This working approach combines petrological analyses, geochemical characterisation and absolute dating of mortars using optically stimulated luminescence (OSL) and radiocarbon dating, stratigraphic analyses of walls, written sources and photogrammetry, and is applied to a study of San Martiño de Armental (Vilasantar, Galicia), an example of a simple, rural parish church in Galicia, in the NW Iberian Peninsula (figure 1).



FIGURE 1

The historical and archaeological context

San Martiño de Armental parish church is located in the village of A Eirexe (Vilasantar, A Coruña), some distance from the local houses, and 90 metres from the closest farm. It stands on a gently sloping hillside overlooking the valleys of *Rego do Bidueiro* and the *Río dos Muíños* (figure 2). The church has the ground plan of a basilica, with a rectangular nave and apse, separated by a buttress with a chamfered end section (figure 3). The apse is higher than the nave and is large, with almost the same dimensions as the nave, as it includes a sacristy adjacent to it (figure 3). It is oriented ESE-WNW and surrounded by a virtually oval wall made of irregular small-to-medium-sized stone blocks, alongside which are a number of niches and tombs that were added at a more recent date.



FIGURE 2

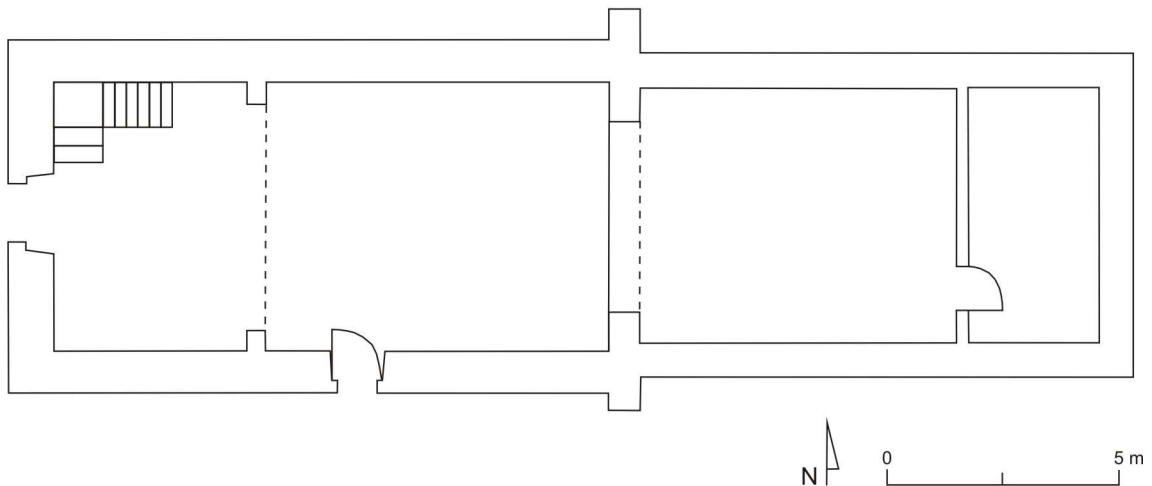


FIGURE 3

The few studies that have examined this church have classified it as a simple example of the Galician rural Romanesque style, datable to around the year 1200, with extensions dating from the modern period, without any outstanding historical or artistic features (VVAA 2013: 149). However, on visiting this church for the first time, in February 2014,

our attention was drawn to the presence of a number of ashlar accumulated in a part of its exterior northern end, which had nothing to do with the rest of the church's external walls (VVAA 2013: 150). In the interior of this same northern end we discovered an ashlar with an unusual inverted epigraph, showing the year 871 AD (+ERA DCCCC et VIIIA) (year 909 of the hispanic era), together with the upper part of a twin stone window, which are typical of the early middle ages in this part of the Iberian Peninsula (figure 4 and 5). Where did all these re-used stones come from? When, and why, were they added to the building?



FIGURE 4



FIGURE 5

We were not able to glean much information from the written documentation. Despite being close to the monastery of Sobrado, which has a large collection of early mediaeval documents (Loscertales 1976), the church of San Martiño de Armental is barely mentioned, only appearing at a late stage in comparison to other churches and villages in its immediate surroundings. It is not until the month of May in 1162 when an "abbas Martinus de Armentar" appears as a witness in two contemporary documents issued by the monastery of Sobrado in relation to the convent of Santa Eulalia in Curtis (Loscertales 1976: vol. I, doc. 184, 185). These are the only references to Armental in documentation prior to the 13th century, indicating that by this time San Martiño de Armental was possibly operating as a monastery under an abbot, probably with a small number of monks, as was the case in much of rural Galicia in the 12th century. Around this same date, mention is also made to a person named "Petro Aloyti from Armentar" (Loscertales 1976: vol. I, doc. 186, 313).

However, we know that the territory around San Martiño de Armental (the Upper Tambre valley) experienced important social and political transformations long time before that first written mention, during the integration of Galicia into the political structures of the Asturian kingdom in the 9th and 10th centuries AD (Isla 1998; Portela 1995). In this sense, it is crucial to understand to what extent the creation of churches played any role in this "state formation process" (Sánchez-Pardo 2015; Baliñas 1992, 2002; Loring 1987) as it happened in other European areas (Innes 2000; La Rocca 2007; Wood 2006). The archaeological analysis of the remains of these early medieval churches can offer

important information to this topic (Quirós and Fernández 2012; Sánchez Zufiaurre 2007; Larrea 2007).

Methodological approach

In an attempt to understand the origins and evolution of this church and the source of the stone material it contains, an interdisciplinary strategy was designed. We first carried out a stratigraphic analysis of its walls in order to comprehend the different phases of the building, followed by a characterisation and dating of the mortars using optically stimulated luminescence (OSL) and radiocarbon dating, to obtain absolute datings for these phases. We finally carried out a petrological analysis with the aim of identifying the origin and source of the different stones used in the building. Using all of the information we obtained, we then produced an interpretation of the evolution of this church's construction within its historical and archaeological context.

2. STRATIGRAPHIC ANALYSIS

2.1. METHODOLOGY

Firstly, with the aim of obtaining a correct geometric documentation of the north and south walls of the nave, as well as of the epigraph and the twin window, we decided to create a photogrammetric model of these elements using Agisoft PhotoScan Pro software. To do so, a series of specific photographs were taken, and the model was then scaled using the measurements of the building made on-site. The result was a 3D model representing the shape and look of the selected elements, with a realistic appearance (with texture, figure 6), and another version without texture that made it possible to visualise other elements, such as inscriptions or carvings.



FIGURE 6

After creating the photogrammetric model of the north and south walls, a stratigraphic analysis was carried out, using the normal methodology based on applying the Harris method to the study of historical buildings (Caballero 1995, Caballero and Escribano 1996), albeit adapted to the extensive working model carried out in the EMCHAHE

project (Sánchez-Pardo, Blanco-Rotea 2014; Sánchez-Pardo *et al.* 2017b): this consists of making a quick recording (Brogiolo 1988: 33; Caballero 2004: 135) which, in the same way as a conventional stratigraphic analysis, is based on differentiating the Stratigraphic Units (SU or UE in the figures) *in situ*, then presenting them in graphic format (figure 7), recording the SU on simplified forms (table 1), creating the stratigraphic diagram (figure 8), and then carrying out the subsequent correlation, synthesis, and dating procedures.

2.2. RESULTS

Based on the stratigraphic analysis, we were able to document four stages of construction.

Phase	Phase name	SU	SU name	Sector	Prior to	Contemporary to	Posterior to
I	Original building made of granite slabs, prior to the 12 th century.	003	Remnants of a wall in the lower central part of the south façade, to the east of the door, made of re-used stone blocks. Between two and four rows still remain; the bottom row juts out like a plinth.	South	001-010, 004		
		009	Remnants of a wall made of re-used irregular stone blocks, to the east of the north wall of the nave. The wide joints are filled with smaller stones; although the materials are generally laid in horizontal rows, and different solutions are used, with shims filling in the gaps.	North	001-010, 008		
II	Romanesque church from the second half of the 12 th century – early 13 th century	001-010	North, south, and west walls of the nave, comprised of irregular ashlars re-used in the west façade, corners, and openings, and of irregularly positioned small-medium sized blocks in the rest of the wall. The northern end includes a final row with corbels, with an overhang. Similar SU001 and SU010.	North, South, and West	002, 004, 012	010	003
III	Extension of the church to the east in the modern age	002?	Top of the south façade of the nave, including a row of eleven corbels supporting an overhang with a truss with a concave covering in the upper section. The corbels and overhang have the same features as those in the north wall.	South			001-010, 004
		004	Buttress between the nave and apse in the south wall of the church, made of granite slabs arranged as stretchers and bonders. The buttress is set into the walls of the nave and the apse, marking the difference in height between both sections.	South	014, 002?	¿002?	001-010, 003
		008	Buttress between the nave and apse in the north façade of the church, made of granite slabs arranged as stretchers and bonders. The buttress is set into the walls of the nave and the apse, marking the difference in height between both sections.	North	005		001-010, 009
		012	Refurbishment of the upper part of the west façade of the church, from north to south. In the southern section it descends to the lintel over the door. Made of irregular small-medium sized masonry blocks, forming pseudo-rows in some sections.	West	006	002?	001-010
		013	Wall located in the lower part of the eastern façade of the apse, made using irregular masonry blocks, tending to form horizontal rows.	East	005?	005?	
IV	Contemporary refurbishment work	006	Curved tile roof. Gabled in the nave, and three-sided in the apse/sacristy.	North, South, East			002, 004, 005, 001-010, 014
		007	Groove cut into the south wall of the apse to insert wiring, filled in with cement mortar.	South			005

Phase	Phase name	SU	SU name	Sector	Prior to	Contemporary to	Posterior to
		011	Repairs made to the upper part of the north façade of the church, using small masonry blocks. Between the 6 th and 7 th corbel counting from the west.	North			001-010
		015	Repairs made to the upper western part of the north façade of the apse/sacristy, associated with refurbishments made to the interior of the church.	North			005, 008

Table 1. List of the SU documented in the church of San Martiño de Armental

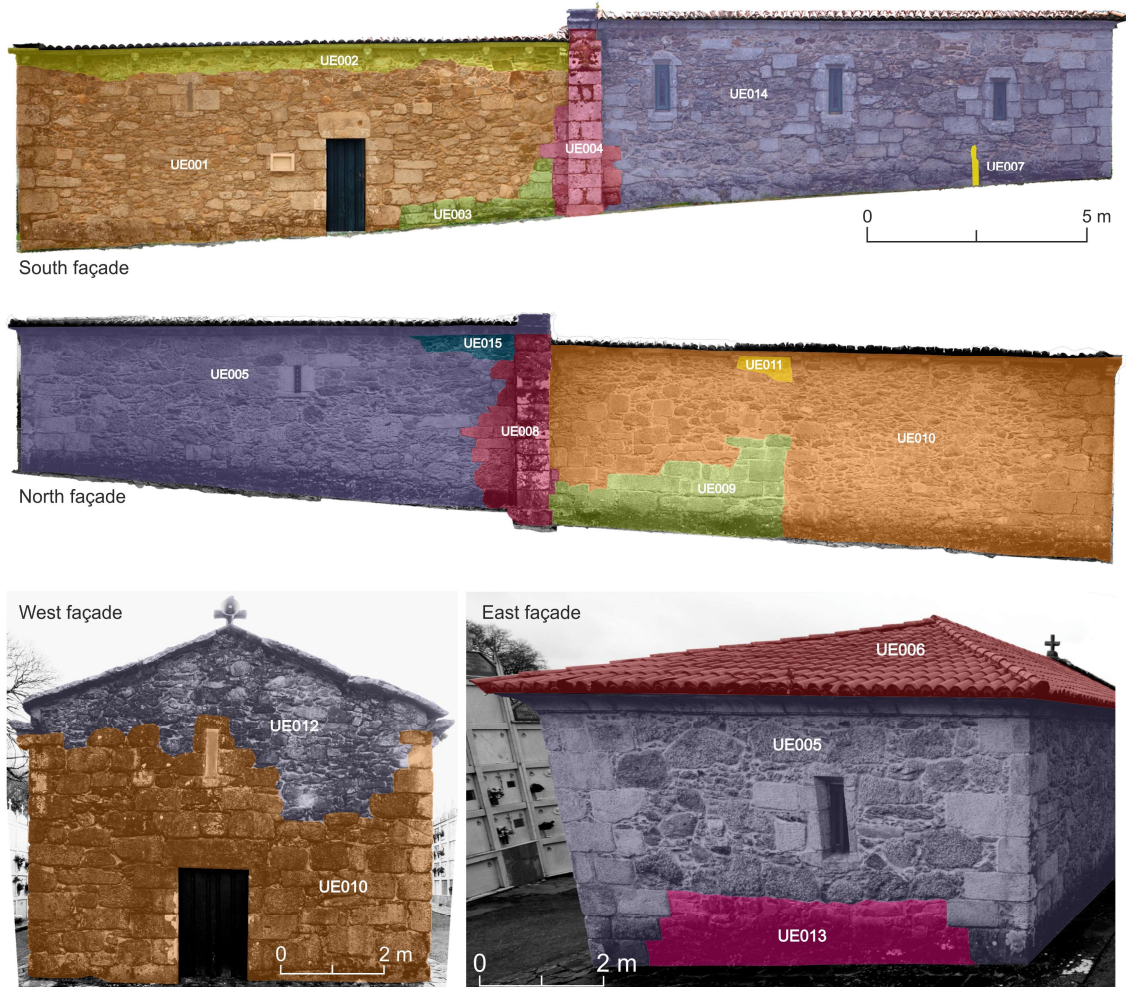


FIGURE 7

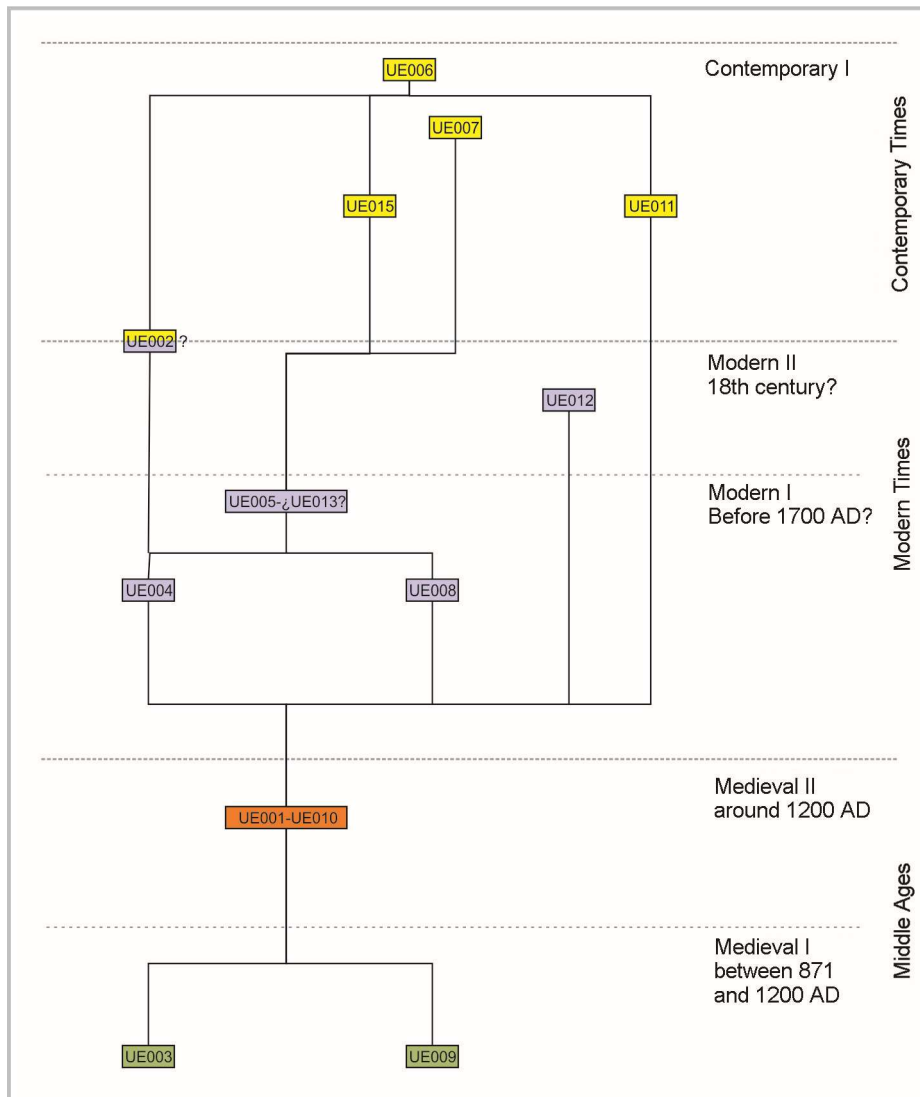


FIGURE 8

Phase I. A building dating from prior to the 13th century

This phase contains the remnants of two walls at the eastern edge of the south (UE003) and north (UE009) walls of the nave, made of re-used, irregularly shaped ashlar and large blocks of granite and quartzite, laid in horizontal rows. The bottom row juts out from the face of the wall. The ashlar are between 1.45m and 0.3m long (figure 9). Re-used sections have been documented: keystones, and stones with lapidary carvings¹, as well as an inverted epigraph and the top part of a window. Due to their irregular nature, angled sections, ships, and double rows were used to keep them horizontal. The joints are wide, filled in with rubble, and covered over with a recent layer of mortar. The end of this northern wall is irregular and intersected by a buttress, UE008, although to the west it is quite regular.

¹ Because of their stratigraphic position, we believe that some of the epigraphic marks (“V”, “P”, “F”) may have been from the stonemasons involved in the subsequent Romanesque phase.

Although there is no physical contact between both walls, due to their position, similar appearance, and the presence of a pedestal jutting out from their base², they are considered to be contemporary. This seems to be the only part that still remains of a building that was incorporated into the Romanesque structure, maintaining its width, and perhaps what was an old place of worship. Its perimeter within the same part of the nave, and the regular western end of the north wall, leads us to consider that the previous building was smaller than the one that can be seen today.

We consider this phase as dating from the 10th to 12th centuries, as an epigraph from 871 was reused, prior to the extension of the church in the early 13th century.



FIGURE 9

Phase II. Romanesque refurbishments from the early 13th century

The majority of the west, north, and south walls of the nave (UE001-UE010) are associated with this phase. The west wall is made of re-used ashlar. Some of the ashlar used in the door are *ex novo*. At the southern end of the façade they are laid out in rows stretching from the corner, although they break up at the height of the door jamb. There are no rows in the northern end. Over the door there is a rectangular arrow slit. The joints are wide, and filled with rubble. The upper part of the façade was rebuilt during a later phase.

The north and south walls are made of jumbled masonry using small to medium sized blocks, with wide joints filled with cement mortar (figure 10). The blocks are of a uniform composition (granites, quartzites, and some quartz and schist). Some of the blocks are re-used. The southern wall has a lintelled door, made of granite with re-used ashlar. Inside, there is an arch with a keystone over the door, which is incomplete and blocked off. There is a similar arrow slit to the one in the western wall. The north and south walls have corbels supporting an overhanging eave, with an incised line in its upper part (figure 10).

² Which does not continue throughout the rest of the structure.

Many of them are cut, and are neither horizontal nor vertical, suggesting that it may have been modified during the refurbishment of the roof carried out in the early 21st century.

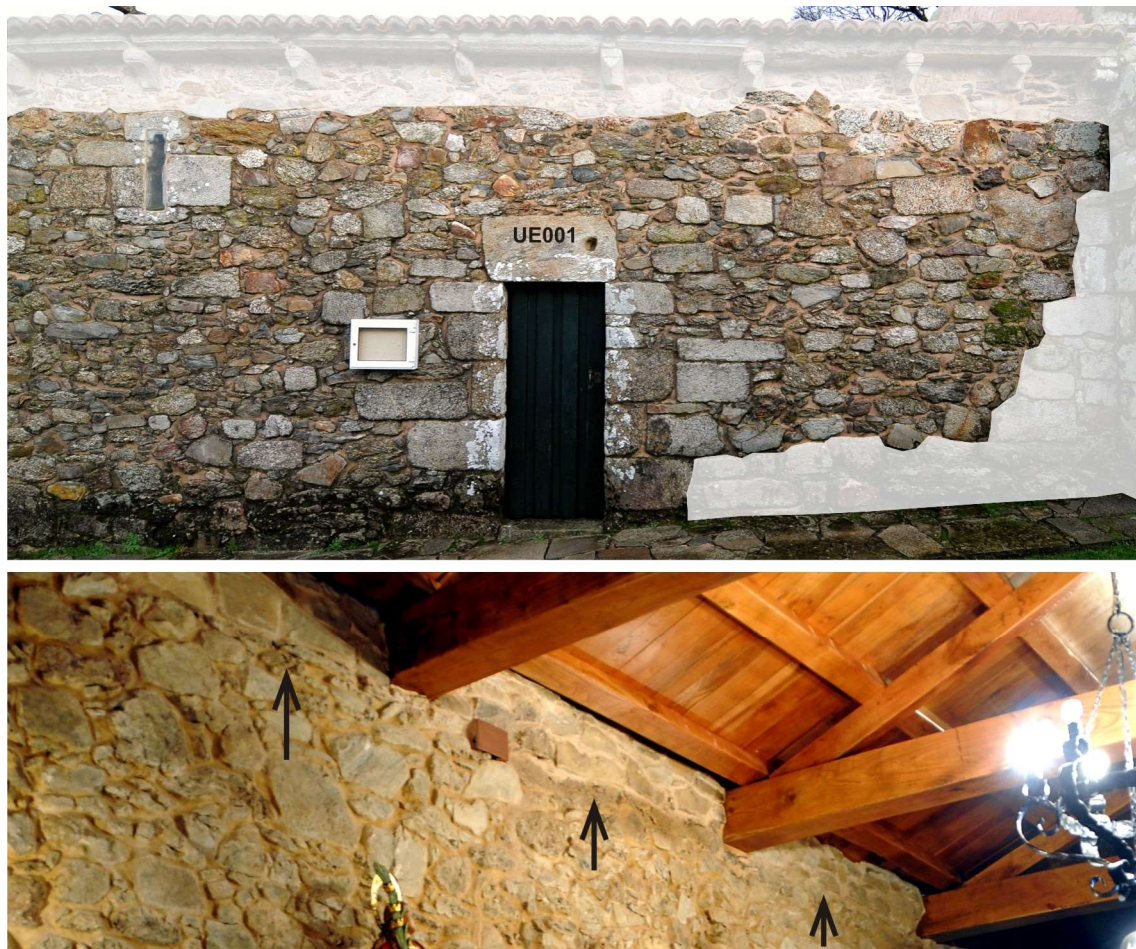


FIGURE 10

The church from this phase, with a single nave, rectangular floor plan, and possibly with a straight apse³, would have been an extension of the previous church towards the west, also raising its height. The façade would have been pentagonal, possibly with a belfry in the southern wall, similar to the near church of Santa María de Cidabela, as seen by the refurbishment of the upper part of the façade (UE012)⁴.

Some authors have dated this phase to around the year 1200 (VVAA 2013: 149). Indeed, this model coincides with other rural churches from this part of Lugo dating from the 12th to 13th centuries (figure 11), which have a single nave made of small masonry blocks and a rectangular or circular apse made of ashlar, also used to make the main façade, door and window openings, and even the upper rows of the nave. The western façade is usually pentagonal, with a central belfry.

³ We are unable to offer data on the apse as it was completely modified in modern times. Our hypothesis is based on other similar models studied in this part of the province of Lugo, like San Pedro de Vilanova (Palas de Reis) or Santa María de Cidabela (Sobrado dos Monxes).

⁴ This hypothesis is based on the fact that the west door is slightly shifted towards the northern part of the façade. We have found this in other churches with side belfries dating from the 12th or 13th centuries, such as San Lourenzo de Carelle (figure 11) whose belfry is on the north side of the west façade, with the door positioned off-centre towards the south side.

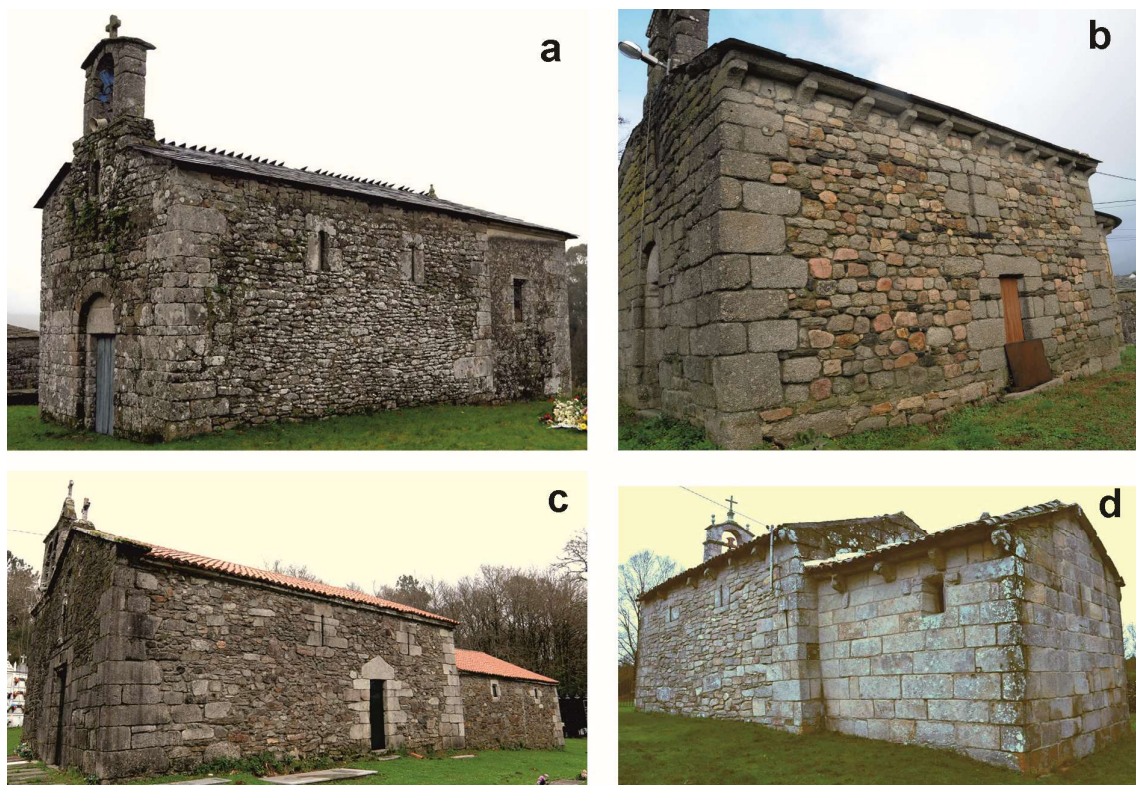


FIGURE 11

Phase III. Transformation of the church in modern times

A major refurbishment was carried out (UE002, UE006, UE007, UE011 and UE015) which resulted in the chancel being extended to the east, including a small sacristy, increasing its height, and also possibly its width⁵. This was done using uneven masonry, with ashlar in the corners, cornices and windows, with some ashlar placed at uneven intervals in the walls, together with irregular medium to large-sized masonry, with large amounts of rubble in the joints. The stone used was mainly granite, quartzite, and quartz. Four windows are lintelled with dual recesses, while the fifth is a sharply recessed arrow slit.

The union between the chancel and the nave includes two buttresses in granite ashlar laid in a stretcher and header bond. Newly cut ashlar is mixed with other re-used ashlar. At the meeting point there is a gable, topped by granite slabs and simple cross on a square pedestal, similar to the one on top of the belfry. This fact has led to the movement of the belfry being dated to the moment when the refurbishment work was carried out in modern times.

The upper part and southern end of the west façade (UE012) were rebuilt using stone blocks. Due to the use of granite slabs, and the different appearance of the masonry to that documented in phase 2, we believe that this would have been contemporary to the modern refurbishments. We do not have enough elements on hand to be able to date this phase with any real precision, although based on the type of capital used on the pilaster

⁵ As we have already said, we do not know what the apse would have been like in previous phases, although if we consider the Romanesque model we used for a reference for other rural churches in the area, the apse would have been smaller than the nave.

supporting the triumphal arch corresponding to this phase, it could be from the 18th century.

Phase IV. Contemporary refurbishments

These correspond to a series of refurbishments carried out inside and outside the church (UE006, UE007, UE011, UE015), on the request of local neighbours in order to continue using the building as a place of worship. The floor inside the church was repaired⁶; a pavement was built around it; the covering mortars were removed, and some areas with leaks were repaired; the roof beams were changed, the roof tiles replaced, and electrical wiring was installed. All of this work was carried out at the start of the 21st century.

2.3. DISCUSSION

The Romanesque building conserves the remains of a wall that may be from a possibly smaller church than the present structure, made entirely of re-used material, dated to between 871 and the early 13th century. Also, it is important to note that the original building re-used several stone blocks, in some cases 145 cm long and 40 cm high (figure 9), as well as decorated sections. This means that there was a greater economic and technological investment in these blocks: while the construction techniques for phase I involved re-using blocks and ashlar, filling the gaps with smaller stones and rubble, phases II and III were made using masonry with some new and re-used ashlar, combined together.

As a result, the stratigraphic analysis revealed a construction sequence, but also raised new questions: what was the absolute chronology of phase I? What was the origin of the ashlar that were re-used in phase I, as well as in the other phases? In order to answer these questions, we decided to characterise and date the mortars, and to characterise the stone materials.

3. CHARACTERISATION AND DATING OF MORTARS

Several mortar samples were characterised and dated following the stratigraphic analysis, in an attempt to date the possible mediaeval phases present in the internal and external sections of the north wall of the church.

3.1. METHODOLOGY

Sampling

A total of 5 samples were taken for characterisation and Luminescence dating: 4 from mortars used in the joints, and 1 from a tile fragment for luminescence dating (figures 4 and 9). Three of the mortar samples were taken from the same wall (the exterior of the north wall: ARM-01, ARM-02 and ARM-03), while one was taken from the interior of the same wall (ARM-08), in the same zone from where the tile fragment was removed (ARM-09). Two additional mortar samples were taken from the same places in the outer wall for radiocarbon dating (ARM 151120U02, ARM-MU160219U03). All of the mortar samples taken for OSL dating were earth mortars. In order to take the samples, it was

⁶ According to a local resident, some 40-50 years ago the floor was made of flattened earth.

necessary to remove a superficial cement mortar using a hammer and chisel. Once this had been removed, it was found that the original earth mortars were still inside the joints, from a depth of approximately ~5 cm. Moreover, 4 rock samples were taken from the immediate surroundings for characterisation (ARM_U04, ARM_U05, ARM_U06 and ARM_U07).

It was not possible to obtain materials that provide a certain degree of reliability for radiocarbon dating, such as carbon or wood. As a result, the dating was made using the organic material from the mortars used as samples. To carry out the luminescence dating, a specific sampling process was carried out, carefully cutting the mortars into cubes which were then removed with a spatula. The materials in the area immediately around the mortar samples (fragments of rock from the blocks in the walls we studied) were also sampled, in order to estimate the gamma radiation rate using a geometric model, although measurements were also made on site using a portable gamma spectrometer. Samples were taken from the same phase for radiocarbon dating, avoiding contamination.

Characterisation of the mortars

The mortars were characterised based on the suggestions of Middendorf *et al.* (2005a, 2005b), adapting them to earth mortars. In earth mortars, it is not possible to estimate the granulometry of the additive, as it does not differentiate between the additive and the bonding material: as a result, the granulometry is carried out on a raw sample, in the same way as the mineralogical and elemental composition analyses. This allowed us to estimate whether the composition of the mortars was the same, or if they possibly had the same origin. During the sampling process for dating, a small amount of the samples was taken for characterisation. In order to characterise the granulometry, wet sieving was carried out.

For the mineralogical characterisation, X-Ray diffraction was carried out, grinding a fraction of the sample and homogenising it so that it could be measured in a SIEMENS D5000 dust diffractometer using CuK_α radiation filtered with Ni. A 2 theta (2θ) sweep was carried out in a range between 3° and 69° at a speed of $1.2^\circ/\text{min}$. The crystalline phases were identified using the JCPDS-ICCD database from 2003.

The elemental analysis was carried out using X-Ray Fluorescence Spectroscopy using the same fractions to obtain the composition of majority and minority elements in a Bruker-Nonius S4 Pioneer X-Ray Fluorescence Spectrometer in a helium atmosphere.

The same samples were recovered and prepared for Inductively Coupled Plasma Mass Spectrometry (ICP-MS), in order to obtain the composition of trace elements. The samples were prepared by fusion with lithium metaborate, mixing the crushed samples with an equal quantity of lithium tetraborate in a carbon crucible, then melting them at 1000°C in a muffle furnace for 30 minutes. After cooling, the resulting fusion was ground and dissolved in 100ml of a solution of 4% HNO_3 /2% HCl_3 and measured by ICP-MS. To do so, a Thermo Scientific™ ELEMENT XR™ ICP-MS was used, which combines a dual SEM mode with Faraday detectors.

OSL dating of mortars

In order to estimate the age by luminescence, the age equation is the ratio between the total absorbed dose measured (estimated as an equivalent dose, or D_e) by luminescence, and the ionizing radiation dose rate of the samples studied and the surrounding materials. The estimated age will correspond to the time that has passed since the dated materials were last exposed to light or heat, before being protected from these factors (Aitken, 1985, 1988). In the case of the mortars, the optically stimulated luminescence (OSL) was used to estimate when the mortars were added (Goedicke, 2003, 2011; Stella *et al.*, 2013; Urbanova *et al.*, 2015; Urbanova and Guibert, 2017). OSL measurements are normally made using quartz granules from the sand used in the additive, at least in lime and sand mortars, although the technique has also been used successfully in earth mortars (Feathers *et al.*, 2008; Sanjurjo-Sánchez, 2016; Sánchez Pardo *et al.*, 2017a), despite the problems that could arise as a result of an incomplete bleaching of the geological luminescent signal, when signal bleaching due to exposure to light prior to adding the mortar has been insufficient, or when there are heterogeneous dose rates, issues that have been explored in a number of studies (Goedicke, 2003, 2011; Urbanova *et al.*, 2015; Urbanova and Guibert, 2017; Sanjurjo-Sánchez, 2016).

At the Luminescence Laboratory of the University of A Coruña, the outermost part of the samples (2-3mm) was removed with extreme care, under controlled red light conditions, using a spatula. In the case of the tile sample, its outermost part was removed using a low-speed rotary saw, cooling the cutting zone with water. Once the samples had been dried, they were carefully crushed using a mortar and sieved to obtain fractions with a grain diameter of 90-180 and 180-250 μm . These fractions were then treated with hydrochloric acid and hydrogen peroxide to remove any possible carbonates and organic matter, respectively. The feldspars and heavy quartz minerals were then separated by density, using a solution of sodium polytungstate with different densities (2.62 g/cm^3 and 2.70 g/cm^3). The quartz fraction obtained was treated with hydrofluoric acid to remove any additional feldspar and the outer layers of the quartz grains, then adding hydrofluoric acid to remove any fluoride that was present. The presence of feldspars was verified by infra-red stimulated luminescence (IRSL).

The samples were measured using an automated Risø DA-15 TL/OSL Reader with a blue diode lighting system (LEDs with a wavelength of 470 ± 30 nm), in order to stimulate the multi-grain aliquots. The signals emitted by the samples were measured by a 9235QA photomultiplier coupled to the equipment, placing a Hoya U-340 filter in the emission window allowing for the passage of a wavelength of 340 ± 80 nm. The samples were also irradiated with a radioactive beta $^{90}\text{Sr}/^{90}\text{Y}$ source mounted on the reader, providing a dose of 0.120 ± 0.003 Gy s^{-1} .

In order to estimate the D_e the single-aliquot regenerative dose (SAR) protocol was applied (Murray and Wintle, 2000, 2003). Small aliquots of around ~ 50 grains were prepared in steel tin-free discs, although the signals were very dim, as the signal to noise ratio was lower than 3/1. For this reason, aliquots of around ~ 150 were used to estimate the D_e . The aliquots were stimulated with blue LEDs for 40s at 125°C after a preheat at 200°C for 10 seconds. This preheat temperature was selected based on previous preheat tests carried out for all of the samples. The response test-dose was measured after heating at 180°C (TL at $5^\circ\text{C}/\text{s}$). The first 0.8 seconds of the OSL signal were used to measure the luminescence, and the last 4 seconds were used to measure the background and subtract it from the signal.

In order to verify any change in sensitivity of the samples, recovery tests were carried out for all of the samples. Firstly, the aliquots were stimulated with blue light for 200 seconds in the OSL reader at room temperature, then applying a beta dose that was approximately equal to the natural dose to the aliquots. OSL signal blanking tests were also carried out in order to estimate the reduction rate of the OSL signal.

The dose rates were estimated by also considering the previous characterisation of the mortars, at least in order to estimate the beta dose and internal gamma dose. The alpha dose was also dismissed, and an attenuation factor of the beta dose was used, due to the use of acid with the quartz grains, which removes their outer layer (Brennan, 2003). The possible internal U and Th content of the quartz grains was dismissed, due to their low content (De Corte et al., 2006; Vandenberghe et al., 2008) of these elements, in comparison to their relatively high presence in the mortars. The materials from the stone blocks in direct contact with and surrounding the mortars were also analysed by XRF and ICP-MS in order to estimate their contribution to the gamma dose, which was estimated based on a geometric model, considering the suggestion of Feathers et al. (2008), contrasting the results with gamma spectrometry measurements taken *in situ*. The conversion factors of Guerin et al. (2011) were used in order to estimate the dose rates.

The cosmic dose was estimated according to Prescott and Hutton (1994), although the cosmic dose on vertical surfaces is complex to estimate (Sanjurjo-Sánchez et al., 2016) due to the topographic shielding caused by angles of more than $\sim 25^\circ$ (Dunai, 2010). On vertical surfaces, the production rate of cosmogenic nuclides is half that of an unobstructed horizontal surface, at least from twice the attenuation distance from the top to the bottom, where it becomes equal to a descent of 50% of the geometric shielding (Dunne et al. 1999). In any event, the majority of studies that have dated mortars by OSL have obtained good results without exploring this issue (Liritzis et al., 2013; Urbanova et al., 2015; Urbanova and Guibert, 2017), with the cosmic dose in this particular study case representing less than 3% of the total dose rate.

Radiocarbon dating

Independent radiocarbon ages were obtained from the organic material found in the two mortar samples. These samples were analysed and measured in a mass spectrometer coupled to an accelerator (Accelerator Mass Spectrometry, AMS) in the laboratory of Beta Analytic (Florida, USA). The ages were calibrated using the Oxcal 4.1 software package (Bronk Ramsey, 2011) based on the calibration curve of Reimer *et al.* (2013).

3.2. RESULTS

Characterisation of mortars

The earth mortars we analysed were very similar, and we did not observe any differences in terms of their granulometry or composition. All of them mainly consisted of fine sand (around $\sim 50\%$) with a small amount of clay and silt (20-27%), with the rest consisting of mortar made of medium to coarse sand. The porosity was similar, varying between 25 and 35%.

In all of the samples, quartz, anortite and muscovite were identified as the main minerals, with the presence of albite and chlorite (clinochlorite) in all of them apart from ARM-08

(figure 12). Kaolinite was also observed in samples ARM-01 and ARM-02, and gibbsite in samples ARM-01 and ARM-03. As kaolinite and gibbsite are produced by the weathering of feldspars, their presence can be attributed to this process in soils from the study area. Chlorite is produced by the weathering of micas, such as muscovite, which means its presence can be presumed to be due to the same process. The low concentrations of these minerals in rocks that have not undergone any extensive weathering, and the overlapping of diffraction peaks with other minerals, are probably the most likely reason why these minerals appear in some samples and not in others. For this reason we considered that differences could not be between the mortars based on the XRD results.

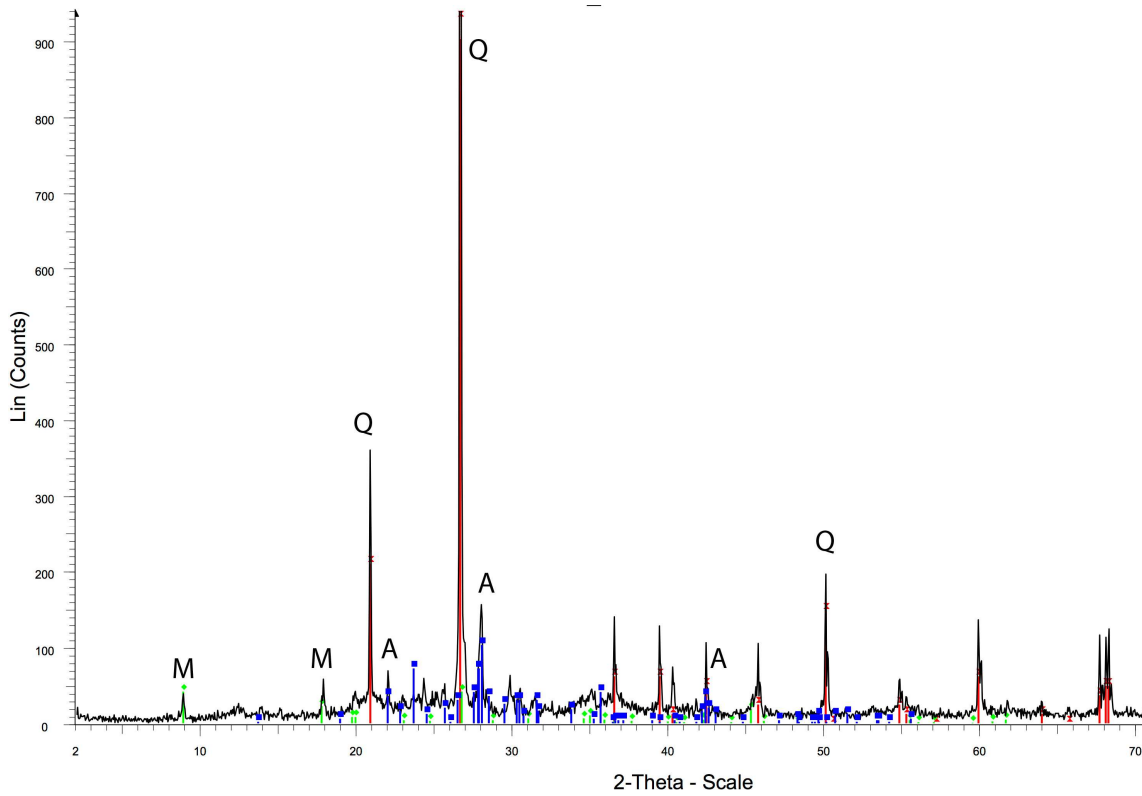


FIGURE 12

The XRF results for raw samples were very similar, revealing similar concentrations of minor and major elements in ARM-01 and ARM-03, with different concentrations in ARM-02 and ARM-08 (table 2). The concentration of these trace elements obtained by ICP-MS coincides with the XRF results (table 2). In order to verify the possible source of the samples, chondrite-normalised rare earth element (REE) patterns were used (Anders and Gravenese, 1989). This pattern is used as a chemical fingerprint to verify the possibly common origin of geological samples such as sediments, or archaeological materials such as pottery (Lipin and Mackay, 1989; Prudêncio *et al.*, 2009). In the case of the samples we studied, the chondrite-normalised REE pattern coincides fully for ARM-01 and ARM-03, while they are clearly different for samples ARM-02 and ARM-04 (figure 13). On observing other parameters, the Eu anomaly for ARM-01 and ARM-03 is similar, in the same way as the total REE and light-heavy REE ratio (LREE/HREE) (table 3), while these were different for the other samples. These values are within the range of edaphic materials observed in Europe (<http://weppi.gtk.fi/publ/foregsatlas/index.php>). On observing the REE pattern for a sample corresponding to one of the types of rocks used in the building (ARM_U06), it was found that samples ARM-09 and ARM_U06 (gneiss) coincided, and are similar to

that of sample ARM-08, although the total REE and LREE/HREE ratio, as well as the Eu anomaly, are different. This could be due to the effect of weathering on the soils used to prepare the mortars, meaning it is difficult to affirm whether these are materials of different origin. The coincidence between ARM-08 and ARM-09, which are materials that are present in the same structure, could indicate that they are contemporary. Attending to the agreement with the REE pattern of one of the studied gneiss samples (ARM_U06), it is possible that the material used for mortars ARM-02 and ARM-08 was collected in an area where the gneiss underlays the soil. This probably corresponds to the church surroundings as gneiss outcrops can be observed there (figure 16). And the geological map shows that it is located on the gneiss-rich area (figure 15).

	ARM-01	ARM-02	ARM-03	ARM-08	ARM-09
SiO2	55.7	56.1	59.1	58.5	59.5
Al2O3	27.1	23.9	24.3	22.0	19.5
Fe2O3	7.4	11.5	7.3	10.1	10.4
K2O	3.5	2.8	3.4	2.9	1.7
MgO	1.5	2.0	1.8	1.9	2.1
Na2O	1.4	0.93	1.6	1.5	1.4
TiO2	1.1	1.2	1.0	0.99	1.6
CaO	0.89	0.64	0.59	1.5	3.0
SO3	0.64	0.096	0.13		0.16
BaO	0.16	0.10	0.16	0.11	0.10
MnO	0.091	0.12	0.079	0.096	0.086
ZrO2	0.055	0.048	0.065	0.049	0.090
ZnO	0.020	0.025	0.021	0.021	0.024
CuO	0.012	0.015	0.014	0.05	0.028
SrO	0.012	0.010	0.011	0.014	0.015
Rb2O	0.011	0.012	0.010	0.014	0.005
P2O5	0.010	0.063		0.017	
Y2O3	0.008	0.014	0.007	0.010	0.007

Table 2. Results of XRF analyses of the mortars and the tile fragment dated by OSL (ARM_09).

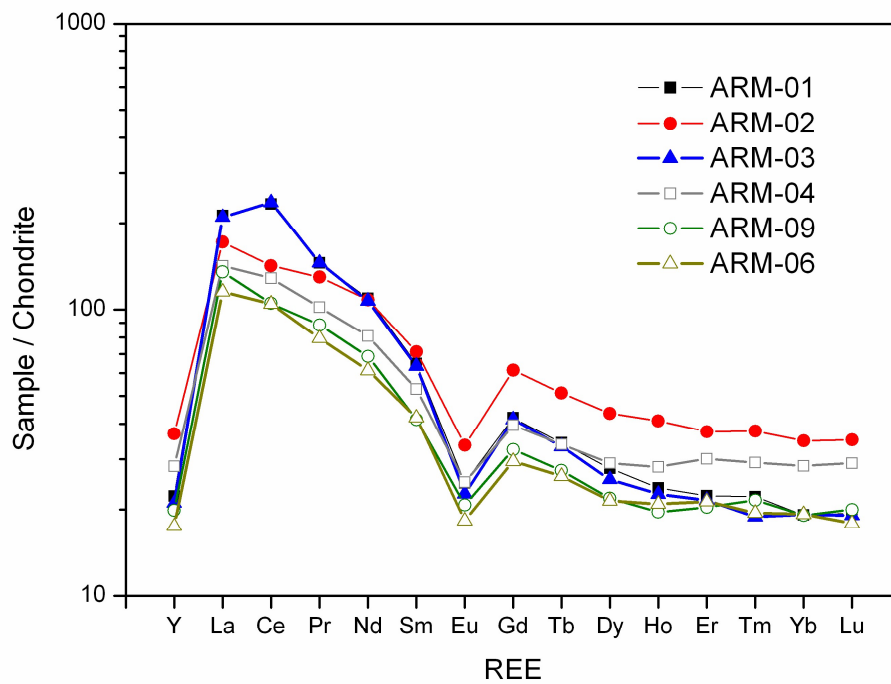


FIGURE 13

Normaliz	ARM-01	ARM-02	ARM-03	ARM-08	ARM-09	ARM_U04	ARM_U05	ARM_U06	ARM_U07
Y	22,3	36,9	21,1	28,3	19,9	5,2	2,6	17,5	12,9
La	212,9	171,8	210,3	142,0	135,4	74,9	29,2	115,4	57,4
Ce	233,5	142,1	236,6	128,7	105,2	24,1	25,5	104,8	65,1
Pr	145,5	129,8	145,5	102,1	88,4	49,4	20,7	79,4	43,5
Nd	109,6	108,1	107,3	81,0	68,6	34,5	15,1	61,3	33,3
Sm	64,8	71,3	63,5	52,8	41,4	19,1	12,8	42,0	23,1
Eu	24,8	33,6	22,7	25,0	20,8	8,4	1,2	18,3	10,2
Gd	41,9	61,4	41,4	39,5	32,4	12,2	8,0	29,5	18,2
Tb	34,3	51,1	33,3	33,9	27,4	8,5	7,1	26,2	15,8
Dy	27,9	43,5	25,5	29,0	21,9	6,8	4,3	21,5	14,7
Ho	23,8	40,9	22,6	28,2	19,6	6,1	2,5	20,9	13,6
Er	22,4	37,5	21,6	30,1	20,4	6,3	1,9	21,3	14,3
Tm	22,2	37,7	18,8	29,2	21,6	8,5	2,4	19,5	13,7
Yb	19,1	34,8	19,2	28,5	19,1	9,7	1,8	19,2	14,6
Lu	19,4	35,2	19,1	29,1	20,0	10,0	1,8	17,9	14,2
LREE/HREE	3,85	2,03	4,00	2,26	2,63	3,17	3,58	2,49	2,06
Eu/eu*	-0,63	-0,60	-0,66	-0,57	-0,55	-0,57	-1,24	-0,59	-0,61
Ce/Ce*	1,30	0,94	1,33	1,05	0,94	0,39	1,02	1,08	1,29

Table 3. Condrite normalized REE concentrations in samples with LREE/HREE ratios and Eu and e anomalies.

Dating of mortars using OSL

In order to estimate the water content, the saturation of the mortar samples was measured during their characterisation, after measuring their environmental humidity. The U and K content of the mortar samples was similar (table 4), although the Th content was more variable: it was similar (around 12 ± 0.6 ppm) for samples ARM-02 and ARM-08, and for the tile fragment (ARM-09), and different from the Th content of samples ARM-01 and ARM-03, which were similar to each other (around 25.0 ± 1.3 ppm). This is reflected in the beta doses of the samples, and it is possible that similarity may be due to them having the same origin. In any event, the dose rates for all of the mortar samples were relatively similar (table 5). The gamma dose estimated *in situ* and based on the geometry was also similar, with the ratio between both estimates oscillating between a range of 0.8-1.2,

having used the geometric estimate in order to estimate the dose rates. This is because the mortar samples were taken from joints at a shallow depth from the surface (just a few centimetres), with the surrounding materials (stone blocks) easily observable in the façade.

Sample	Material	W (%)	U (ppm)	Th (ppm)	K (%)
ARM-01	Mortar	10±2	2.81±0.14	24.4±1.22	2.91±0.03
ARM-02	Mortar	10±2	3.44±0.17	12.25±0.61	2.32±0.02
ARM-03	Mortar	10±2	2.84±0.14	26.4±1.32	2.82±0.03
ARM-08	Mortar	15±2	3.57±0.18	12.0±0.60	3.82±0.04
ARM-09	Tile fragment	8±1	2.42±0.12	13.05±0.65	4.40±0.04
ARM_U04	Rock	2±0.2	3.93±0.20	20.20±1.01	2.82±0.03
ARM_U05	Rock	7±1	4.32±0.21	6.05±0.30	2.41±0.02
ARM_U06	Rock	5±1	2.04±0.10	16.65±0.83	2.41±0.02
ARM_U07	Rock	5±1	2.1±0.11	19.85±0.99	1.41±0.01

Table 4. Estimated radionuclide and water content for the samples analysed.

Sample	Beta DR (mGy/a)	Gamma DR (mGy/a)	Cosmic DR (mGy/a)	DR (mGy/a)
ARM-01	2.79±0.60	1.21±0.08	0.12±0.01	4.13±0.23
ARM-02	2.23±0.48	1.19±0.06	0.12±0.01	3.55±0.22
ARM-03	2.79±0.60	1.17±0.09	0.12±0.01	4.08±0.23
ARM-08	3.03±0.44	0.89±0.22	0.12±0.01	4.04±0.29
ARM-09	3.53±0.48	0.91±0.15	0.12±0.01	4.56±0.22

Table 5. Dose rate of samples dated by OSL.

The OSL signals observed in the mortar samples were similar, and weak. The brightest signals were observed in ARM-03 and ARM-08, with the natural signal fluctuating between 60 and 300 cts. Despite this, the decay of the signal was fast, bleaching 80% of the initial signal after stimulating for 1-2 seconds with blue light in the OSL reader. The fastest signal was observed for sample ARM-08, with around 20% of the initial signal remaining after 1 to 1.5 seconds of exposure time, as demonstrated by the blanking tests. Therefore, the signal to noise ratio was similar for all of the samples, being low and in high deviations for the estimated. The D_e were estimated based on a significant number of accepted aliquots (30-44) according to the requirements of the SAR (Wintle and Murray, 2000, 2003). The distributions obtained for the D_e of the aliquots that were measured were asymmetrical and poorly targeted, as can be seen in the histograms and radial plots (Figure 14), providing overdispersion values obtained by the Central Age Model (CAM) of more than 30% for all of the samples. In these types of cases, it is advisable to use the Minimum Age Model (MAM) proposed by Galbraith *et al.* (1999). This is because using the CAM can lead to an overestimation of the age, obtaining ages of more than 2000 years old if it is applied to the samples we studied in this case. We can suppose that these asymmetrical distributions were a result of a partial sweep of the residual signal, or a total sweep of some quartz grains and an incomplete sweep of others, while preparing the mortar before being used in the construction of the walls. The dose recovery tests provided a good recovery ratio of around ~ 1.0 , although with large deviations, close to ± 0.1 due to the low signals. Using MAM resulted in obtaining ages that were consistent with those expected (table 6).

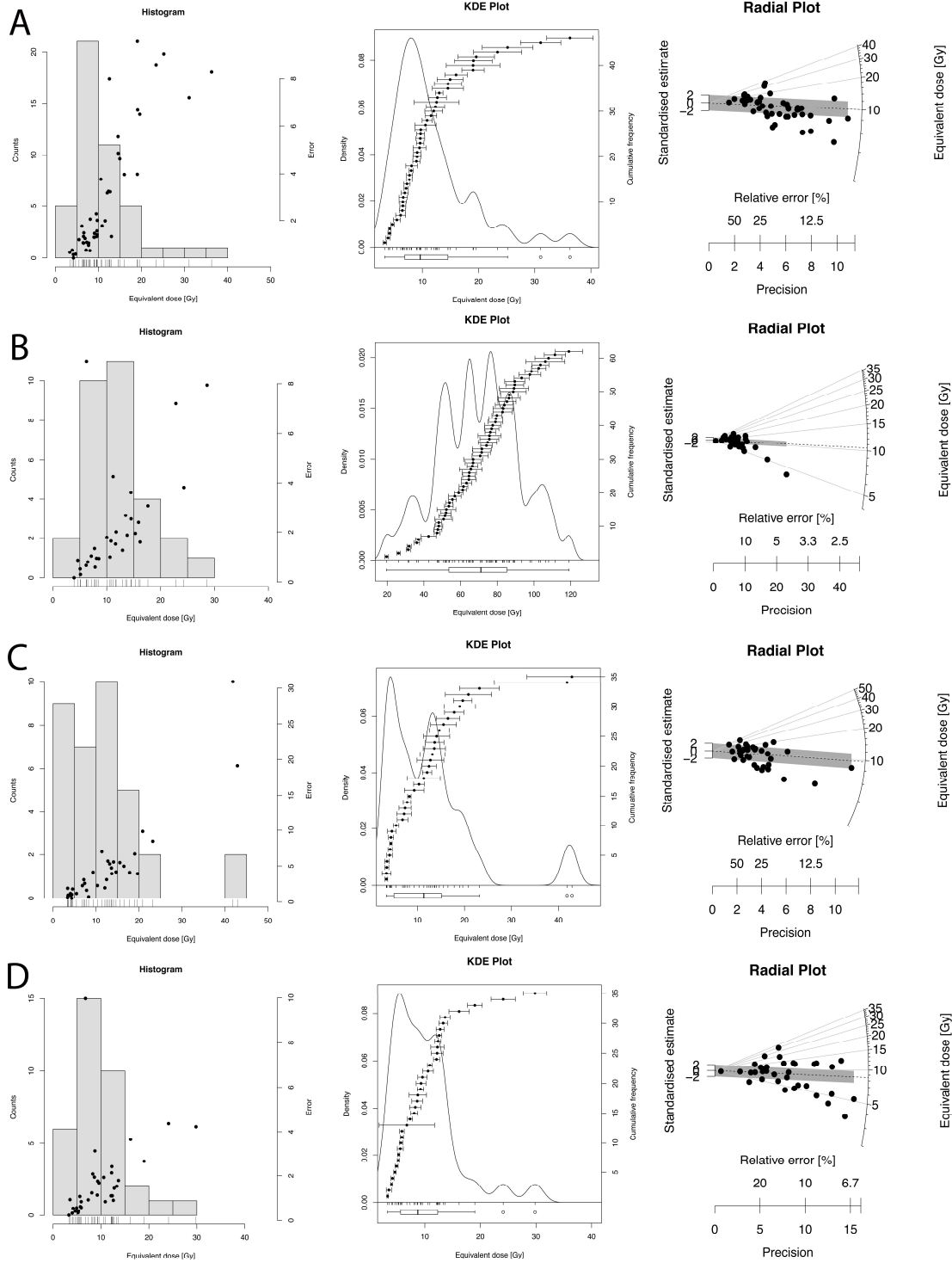


FIGURE 14

Sample	Grain size (μm)	N	De (Gy/)	Overdisp (%)	Age Model	Age (a)	Age DC
ARM-01	90-180	44	4.20 ± 0.35	47.8 ± 6.0	MAM	1018 ± 103	997 ± 103
ARM-02	90-180	30	3.94 ± 0.17	46.5 ± 6.8	MAM	1111 ± 85	904 ± 85
ARM-03	90-180	35	4.19 ± 0.33	53.3 ± 8.7	MAM	1027 ± 99	988 ± 99
ARM-08	90-180	35	3.34 ± 0.32	51.4 ± 6.8	MAM	827 ± 100	1188 ± 100

ARM-09	90-180	42	4.12±0.17	-	-	903±58	1112±58
--------	--------	----	-----------	---	---	--------	---------

Table 6. OSL ages obtained for the samples studied

Radiocarbon dating

The radiocarbon age obtained for the organic material from the mortar samples (table 7) was older than expected, considering the limited archaeological and historical information that was available to us. These ages do not coincide with each other, although the $\delta^{13}\text{C}$ (‰) obtained for them indicate that this organic material comes from relatively unaltered plant remains in the ground, meaning it must be older plant material from floors created before the mortars, results which do not coincide with the datings provided by OSL.

Sample	^{14}C Age (uncal)	$\delta^{13}\text{C}$ (‰)	Sample Code	Cal Age
ARM 151120U02	1550 ± 30	-25.0	Beta - 425502	420-575 DC
ARM-MU160219U03	3770 ± 30	-24.5	Beta - 436839	2285-2060 BC

Table 7. Radiocarbon ages obtained by AMS.

3.3. DISCUSSION

If we only consider the results from the datings and the characterisation of the mortars, it is not easy to obtain a clear construction sequence for the building, although if we contrast these data with the stratigraphic and petrological analysis we can suggest a common explanation, as we will see later on in this paper. The radiocarbon dating did not provide applicable results, despite the fact that the organic material that was found had favourable characteristics, as it was plant matter that had undergone few changes in the soil from where the raw material was taken. The explanation of this result goes beyond the scope of this study.

The chronology of the mediaeval phases of the building we studied was obtained by OSL dating. The resulting ages were similar, although they did not coincide for all of the samples, with a clear difference between the samples taken from the façade and those taken from the internal walls. The samples from the façade (ARM-01, ARM-02 and ARM-03) jointly provided an age of between the end of the 9th century and the end of the 10th century. This coincidence concurs with the characterisation that was carried out, indicating that the materials used for both mortars had the same origin, and that they were the same mortar. In the case of sample ARM-02, whose analysis revealed differences with the previous two mortars, the age range was from the start of the 9th century through to the end of the 10th century (819-989 AD). Despite this difference in age, the ages overlap extensively, and we cannot affirm that the ages are significantly different. A review of these results with the stratigraphic and petrological analysis will help us to resolve this issue later on.

In the case of the materials dated from the internal wall, their age also coincides, although they are different types of materials: one mortar, and a tile fragment. In any event, it is important to bear in mind that tile fragments were normally re-used in buildings, leading to an overestimation of their age; in this case, the most reliable dating is ARM-08, which indicates that the mortar was laid between 1088-1288 (1188±100). This date coincides with the proposed datings for the construction of the Romanesque phase of this church, around 1200 A.D (VVAA 2013: 149).

4. GEOLOGICAL AND PETROLOGICAL ANALYSIS

It was necessary to identify the lithologies used in the construction of San Martiño de Armental in order to discover the sources of the stone that was used. To do so, both geological and petrological techniques were applied, in particular studying the local cartography, macro and microscopic visual identification, and chemical and mineralogical analyses.

4.1 GEOLOGICAL CONTEXT

The parish of Armental is shown on Page 71 of the Spanish national geological map (IGME, 1981), and belongs to the municipal district of Sobrado dos Monxes (Figure 15). The geological context corresponds to the Galician domain of *Trás os Montes*, within the Central Iberian Zone of the Iberian Massif, characterised by the presence of granitic rocks and different types of metamorphic complexes associated with the oceanic suture zone during the Hercynian Orogeny (Arenas *et al.* 2004). Locally, the most important structure is the antiform of Sobrado, a tectonic window with outcrops of medium and high grade metamorphic rocks, and ultramafic rocks from deep source regions.

The church stands on what is known as the Corredoiras Unit, characterised by an abundance of medium-pressure metamorphic rocks, whose lithology ranges from milonites, schists, and granulites, to gneisses. The gneisses are precisely the rocks with the largest number of outcrops, forming an extensive strip that surrounds the central part of the antiform. These rocks normally appear in the form of metric boulders throughout the soils in the area. The approximate age is 500 million years (Abati *et al.* 1999).

SOBRADO ANTIFORM

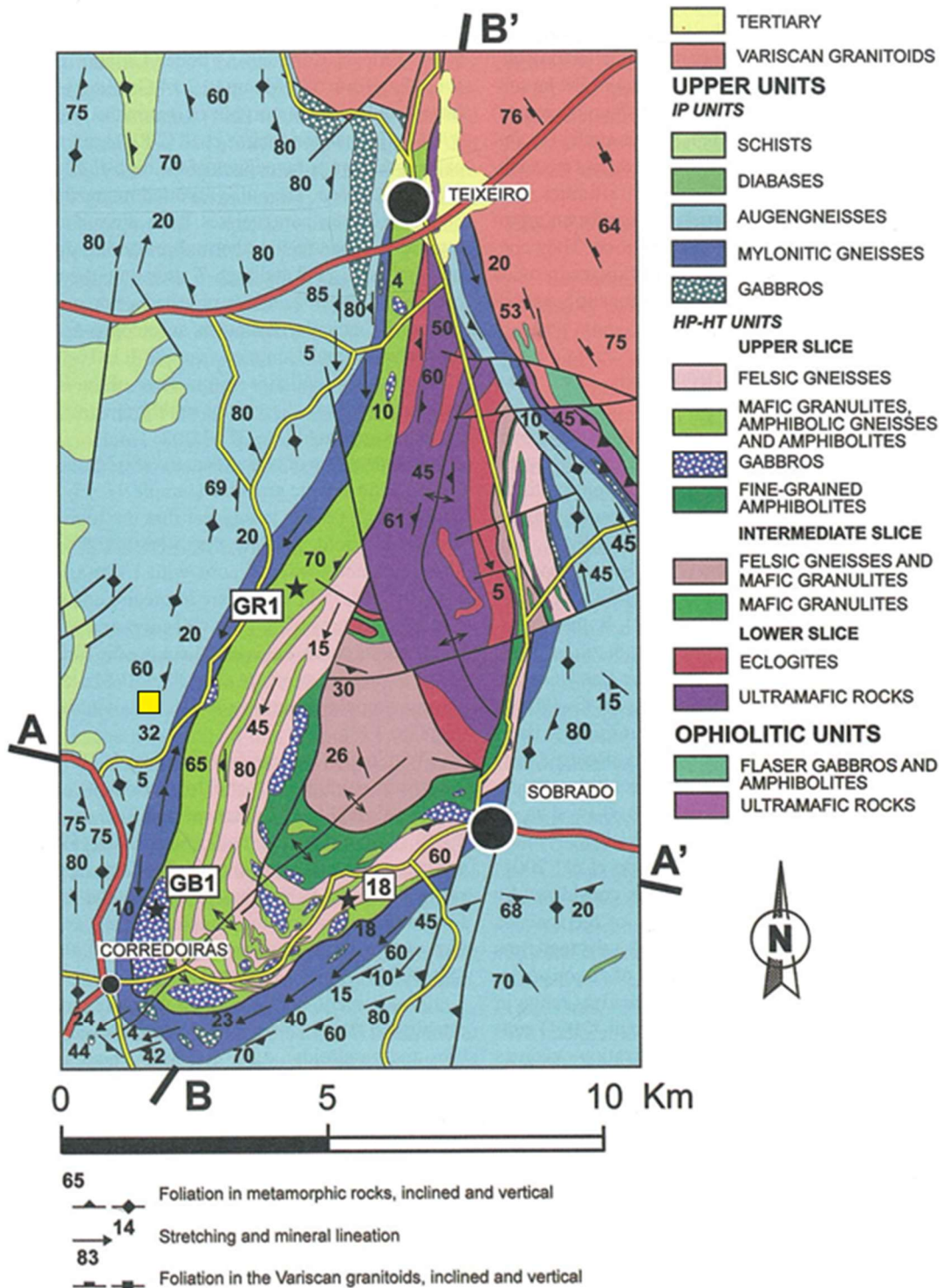


FIGURE 15

4.2. METHODOLOGY

Sampling

In order to obtain the samples from the church, two field trips were organised in order to identify the most abundant materials in the walls being studied, and their position within the surrounding structure. The samples were taken from the courtyard of the church, based on the dominant lithologies in the different construction phases we identified. In an initial analysis, a series of lithologies were observed in the walls: schists, quartzites, gneisses, and granitoids, the latter two being the most abundant. In the area identified as being pre-Romanesque, there is a larger amount of granitic rocks, while gneisses are more frequent in the subsequent phases.

The most common rocks correspond to two types that can be distinguished by their macroscopic appearance:

- 1) Stones with a metamorphic texture, either with clearly marked foliation (M-1 and M-3), or with feldspar porphyroblasts (M-2)
- 2) One stone with a finely grained granitic appearance, with a predominance of leucocratic minerals (M-4 and M-5).

Analytical methodology

Chemical and mineralogical analyses were carried out in order to identify their composition and mineralogy. The chemical composition was identified using X-Ray Fluorescence (XRF) using a MALDI-TOF Voyager STR-DE device from AB. The mineralogy was identified by X-Ray Diffraction (XRD) using SIEMENS D5000 device. Both analyses were carried out at the facilities of the General Research Service of the UDC. A thin layer was taken from each of the samples for analysis using a Nikon 512005 optical polarising microscope. A Nikon H550S magnifier was also used to observe macroscopic details of the texture of the stones.

4.3. RESULTS

Chemical and mineralogical analyses

The mineralogical analyses obtained by XRD revealed that in all of the samples, the main minerals were quartz, anortite and albite, with biotite, diopside and riebeckite as accessories, and also with muscovite in M-5 (table 8).

	M- 1	M- 2	M- 3	M- 4	M- 5
SiO₂	65.2	65.3	70.2	69.7	64.2
Al₂O₃	18.4	17.2	16.0	16.9	19.0
K₂O	4.0	2.1	4.0	5.2	3.0
Na₂O	3.8	5.6	5.0	5.2	4.6
Fe₂O₃	3.7	4.0	2.0	0.97	4.2
CaO	2.0	3.3	1.6	0.61	2.1
MgO	1.1	1.1	0.40	0.26	1.3

TiO₂	0.68	0.64	0.36	0.12	0.73
P₂O₅	0.47	0.13	0.15	0.54	0.41
BaO	0.25	0.15	0.081		0.19
MnO	0.046	0.046	0.028	0.013	0.055
ZrO₂	0.032	0.043	0.037	0.008	0.038
SrO	0.026	0.028	0.012	0.006	0.025
ZnO	0.009	0.008	0.003	0.008	0.011
Rb₂O	0.008	0.005	0.013	0.033	0.007
CuO	0.007	0.008	0.006	0.005	0.007
SO₃					0.054

Table 8. Chemical composition by XRF of the samples taken

Macroscopic analysis

Samples M-1 and M-3 were characterised by having a distinctly crenulated foliation. The minerals were located in intensely deformed layers with hardly any crystals larger than 3 mm, except in the case of the feldspars, which could form porphyroblasts of up to 7 cm.

In sample M-2, the foliation was less developed, with quartz and feldspar crystals measuring several millimetres. In this case, the largest crystals were also feldspars, forming aggregates measuring several centimetres.

Samples M-4 and M-5 had a different appearance. The predominant texture was a fine grain, especially in M-4, with millimetric crystals without any preferred arrangement. In M-5 we observed a larger grain size and the presence of small muscovite crystals. The darker minerals were less abundant than in the previous samples.

Microscopic analysis

A thin section analysis of each of the samples provided further mineralogical and textural details of each particular lithology (fig. 16).

Special attention should be drawn to the similarity between samples M-1 and M-3, as both have a porphyric-nematoblastic texture, with bands of biotite and amphibole surrounding the quartz and feldspar crystals. These include frequent transformations of biotite to chlorite, with aggregates of these micas in kink textures.

In M-2 the texture was granoblastic, with quartz crystals with undulose extinction, feldspars, and plagioclases in mosaic. Some of these feldspars were seritised. The biotite did not form bands as in the previous samples, although there was some degree of transformation into chlorite.

Samples M-4 and M-5 contained feldspars and plagioclases in idiomorphic and subidiomorphic crystals, while the quartz also appeared in allotriomorphic crystals. In general, the texture was hypidiomorphic. M-5 contained small subidiomorphic crystals of muscovite.



FIGURE 16

4.4. DISCUSSION

The results obtained from the XRF analyses revealed typical values for acidic igneous rocks in a broad sense, which were predominantly granodiorites (Krauskopf & Bird, 1995). This idea is reinforced by the mineralogical composition, which is rich in quartz and feldspar.

The macro and microscopic visual study made it possible to identify metamorphic textures that categorised samples M-1, M-2 and M-3 as orthogneisses. The values obtained coincide with those proposed by authors such as Andonaegui et al. (2012) or González Cuadra (2007) who classify these rocks as granodioritic gneisses with a different type of deformation. As a result, we found examples with a clearly crenulated foliation, and others with a weak deformation. Highly deformed or otherwise, these rocks can be found in numerous outcrops close to the church (Figure 17).

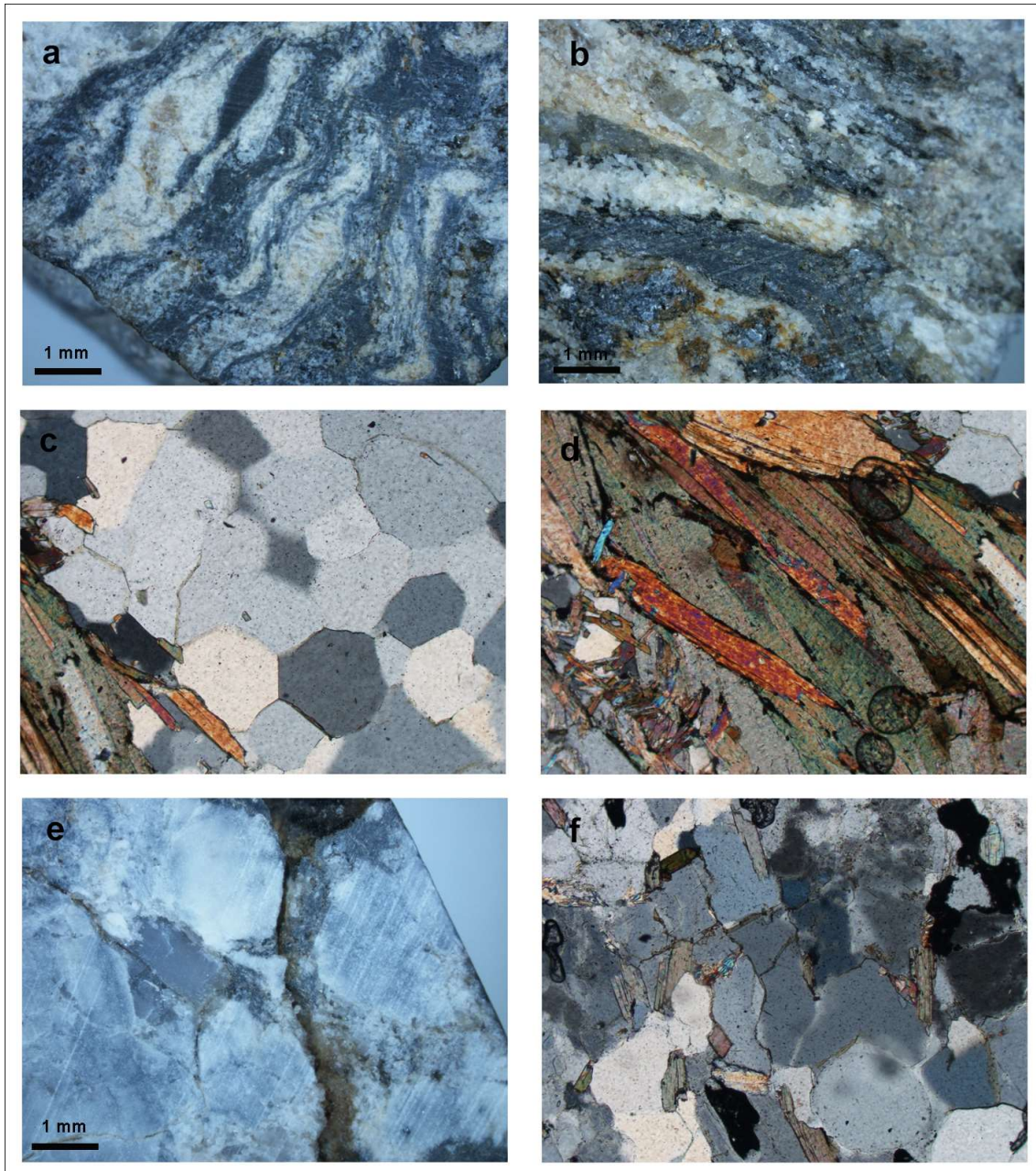


FIGURE 17

Samples M-4 and M-5 correspond to granitic rocks with little deformation. In the area there are occasional outcrops that appear as enclaves within the Corredoiras Unit, and at a distance of less than 10 km to the north-east there is a large outcrop of granodiorites.

Therefore, we can conclude that in the pre-Romanesque phase of construction, mainly granitic rocks were used, while in the subsequent phases mainly gneiss materials typically found in the area were used, as well as granodiorites from nearby zones. In both cases, the materials came from local sources, although the materials from the pre-Romanesque phase came from farther away than those used in the Romanesque, modern, and contemporary phases.

5. INTERPRETING THE RESULTS: A MORE COMPLEX DEVELOPMENT THAN EXPECTED FOR SAN MARTIÑO DE ARMENTAL

The combination of the stratigraphic, petrological, and mortar analysis revealed a far greater complexity than initially thought for the composition of the church of San Martiño de Armental. In this section, we will combine the results of all of these analyses in an attempt to reconstruct the development of this church, and the origin of its construction materials.

Firstly, we confirmed, through the stratigraphic analysis and by the OSL dating of sample ARM-08 from the internal wall, that the church has a Romanesque phase, probably built around the year 1200, as suggested by previous studies. However, part of this Romanesque phase is built over a previous stratigraphic layer, which is still preserved at least in the outer northern wall. As we have seen, the characterisation and dating of three mortars from these remains (ARM-01, ARM-02 and ARM-03) confirmed their early medieval dating, providing four explanatory hypotheses:

1/ The three mortars dated from the external wall would correspond to the same phase, when the three chronologies obtained overlapped (894-989 AD) in which two types of earth mortars from different sources were used, as indicated by their geochemical composition.

2/ The mortars would correspond to two different construction phases (one between 819 and 989 AD, and another between 894 and 1097 AD), in coherence with their different geochemical composition.

3/ The age of the mortar ARM-02 would really reflect the date when the building was constructed (819-989 AD) and the other two indicate a moment when the original mortars in the joints were replaced at a subsequent time (894-1087 AD), meaning there was only one single construction phase.

4/ The sample ARM-02 would correspond to the remnants of an old mortar from the 9th – 10th centuries, which remained attached to the ashlar when it was re-used in the 10th – 11th centuries. This could also possibly apply to sample ARM 151120U02, dated to the 5th – 6th centuries by radiocarbon dating.

The stratigraphic and petrological analyses do not support hypothesis 2, as no construction differences were detected that would suggest different phases between the locations from where samples ARM-01, ARM-03 and ARM-02 were taken. Also, considering the type of mortar, hypothesis 4 seems highly unlikely (that there are remnants of older mortars adhered to the blocks), as because this is earth mortar, once the original building was demolished to which the materials re-used in Armental belonged, it would have been very difficult for this mortar not to have fallen off. Nor does the stratigraphic analysis support hypothesis 3, as the date of the epigraph re-used in the interior supports a dating *postquem* to 871 for this re-use, which coincides much more closely with the dates for samples ARM-01 and 03 than with ARM-02.

For all of these reasons, we consider hypothesis 1 as being more likely, with the three samples of external mortars corresponding to the same pre-Romanesque phase, dating from between 894 and 989 AD. In any event, the other hypotheses would not excessively alter the panorama, as we would still be dealing with the remains of a pre-Romanesque church, although it would be slightly older (from around the 9th century, possibly corresponding with the date of the epigraph), with some type of refurbishment work carried out (either building work, or simply repointing of the brickwork with mortar) in the 10th – 11th centuries.

In any event, returning to hypothesis 1, which we consider to be the most likely, we would be dealing with an old building made of granite ashlar that were mainly re-used, including an epigraph with the date 871 and a twin window, typical of early medieval buildings from the 9th and 10th centuries in the north-west Iberian Peninsula. We do not know the origin of all of the material that was re-used in the building in the 10th century, but it is possible that it came from a previously existing church that was consecrated in 871 that stood on the same spot or in the immediate surroundings, as we have verified that this type of granitic rock can be found easily in a radius of 10 kilometres. In this case it is important to note that the nearby monastery of Santa María de Mezonzo, 2 kilometres away in a straight line and which also contains a number of pre-Romanesque remains (VVAA 2013: 678), was consecrated precisely in the year 871 (Freire 1998: 777-779; Loscertales, 1976: vol. I, doc. 52). For this reason, we cannot rule out the possibility that these re-used materials (or at least part of them) came from this old monastery, or at least from one of its satellite churches that was founded at the same time, such as San Pedro de Présaras (Loscertales, 1976: vol. I, doc. 52).

Whatever their origin, these were good quality materials and construction techniques, using ashlar (*ex novo* or re-used), something that indicates a large economic investment (Utrero and Sastre 2012), at least in comparison to the subsequent phases of San Martiño de Armental, characterised by the use of stonework and the use of masonry techniques (Figure 18). We also know that the geological origin of both stone and mortar was local. Therefore, based on the material data and written documentation, we can propose that around the end of the 9th century, a series of elites operated in this area by building churches with a relatively good architectural quality. These elites were able to mobilise economic resources and a production chain of some size that went beyond the local sphere, involving aspects such as the supply of materials, and the involvement of specialised personnel with technical skills (Quirós and Fernández 2012: 33-42).

This fits in well with what we already know about the historical context of this area in the second half of the 9th century. This was a time when Galicia was incorporated into the kingdom of Asturias, and its accompanying process of political and territorial reorganisation (Baliñas 1992, 2002; Portela 1995, 2002; Isla 1992). Against this backdrop, the founding of churches and monasteries became an interesting strategy of power for local and foreign elites, in order to seek a favourable position within this context of instability and transformations (Innes 2000: 16-50; Sánchez-Pardo 2015). The churches made it possible to intervene in the process of taking control of the territory, by creating a series of landmarks that prevented the disintegration of family properties, made it possible to capture new property and donations, and which helped to ideologically underpin their control through the prestige and legitimacy of the church (Loring 1987: 89; Wood 2006; Laroocca 2007). Furthermore, the churches and monasteries allowed their founders to forge new links, especially through donations, with other aristocratic groups, and to build relationships with the monarchy (Innes, 2000: 16-50; Davies, 2007; Sánchez-Pardo 2015).

We do not know why the remains of some of these churches from the year 871 were demolished shortly afterwards, between 894 and 989, in order to build (or re-build) the church of San Martiño de Armental. There may be numerous reasons, including the destruction of the previous building due to some type of damage, imperfection, or instability. Amongst other possibilities, we know from a document written by Bishop

Pedro in 995, that in the second half of the 10th century (probably in the year 968), a Viking attack led to the looting and destruction of the nearby monastery of Santa Eulalia de Curtis "and other neighbouring churches". One hypothesis is that this was when the building was destroyed that provided the good-quality stone material that was re-used in San Martiño de Armental between 894 and 989. In any event, what is clear is that at this time, following the disappearance of the authorities and context that had been responsible for paying for the first, high-quality building, then local, more economic solutions were used that did away with the need to extract new material. Perhaps the transition of the political dynamics of the kingdom of Asturias-León towards more southerly regions brought an end to this especially fruitful episode of relations between local and supra-local spheres in this part of the Upper Tambre region, which would also explain why this context of major investments in rural churches in this area came to an end.

The same sensation is obtained when analysing the following phases of the church, which mainly used irregular masonry made of local materials. We know from the dating of the mortar inside the church by OSL that at some stage between the 11th and 13th centuries (coinciding with the Romanesque chronology of c.1200AD proposed by investigations from the perspective of the history of art for this church), it was decided to extend the church of San Martiño de Armental in the new Romanesque style (Figure 18). Perhaps the aim of this refurbishment was to make space for a larger number of worshippers, due to demographic growth in the 12th century and an increase in excess agricultural produce, also associated in part with the expansion of the nearby Cistercian monastery of Sobrado (Pallares 1979: 151-156). However, during this refurbishment it was decided to leave part of the external walls with ashlar re-used from the previous pre-Romanesque church, while filling in the joints with new mortar, and building the rest in masonry made of locally sourced stone, with the exception of the façade and cornerstones, which were made of granite ashlar, including some blocks that were clearly re-used. These were very simple building solutions, indicating that very little resources were invested in the building of this Romanesque church, unlike the nearby church of Santa María de Mezonzo, built in delightful Romanesque style in the late 12th century .

In modern times, the Romanesque building was extended, demolishing the chancel and extending the nave towards the east. Simple, economic construction techniques were also used for this new refurbishment, using locally sourced masonry that would indicate a relatively low investment on the part of those who commissioned the work (Figure 18).

**Modern times
(17th-18th centuries AD)**



**Romanesque
(ca. 1200 AD)**



**Early medieval
(9th-10th centuries AD)**



FIGURE 18

6. CONCLUSIONS

By combining a study of the archaeology, mortars analysis and dating, stone characterization, and written documentation pertaining to a simple rural church, it has been possible to reveal that it has a much more complex history and evolution than previously thought. Thanks to this multi-disciplinary approach, whose cost was relatively low in comparison to the results it provided, we now know that the re-use of materials is something that can continue over several phases of use, and also be an interesting reflection of the different construction techniques used and level of economic investment made by those who ordered the work to be carried out. Finally, we must remember that this is only one example, as there are many other Romanesque churches around the church of San Martiño de Armental with re-used ashlars in their walls (i. e. Santa María de Cidadela, San Lourenzo de Carelle, San Vicente de Curtis or Santa Eufemia de Montes) that could provide us with valuable information about their historical evolution, if we study them from a wider perspective than that which has been used to date.

REFERENCES

- Abati J, Dunning GR Arenas, R., García, FD, Cuadra, PG, Catalán, JRM (1999) Early Ordovician orogenic event in Galicia (NW Spain): evidence from U-Pb ages in the uppermost unit of the Ordenes Complex. *Earth and Planetary Science Letters* 165 (2): 213-228
- Anders E, Grevesse N (1989) Abundances of the elements: meteoritic and solar. *Geochim Cosmochim Acta* 53:197–214. [https://doi.org/10.1016/0016-7037\(89\)90286-X](https://doi.org/10.1016/0016-7037(89)90286-X)
- Andonaegui P, Castiñeiras P, González Cuadra P, Arenas R, Sánchez Martínez S, Abati J, Díaz García F, Martínez Catalán JR (2012) The Corredoiras orthogneiss (NW Iberian Massif): Geochemistry and geochronology of the Paleozoic magmatic suite developed in a peri-Gondwanan arc. *Lithos* 128-131:84-89 <https://doi.org/10.1016/j.lithos.2011.11.005>
- Arenas R, Martínez Catalán JR, Díaz García F (2004) Zona de Galicia-Tras-os-Montes. In: Vera JA (ed.) *Geología de España*. Sociedad Geológica Española-IGME, Madrid, pp. 133-165
- Baliñas Pérez C (1992) Do mito á realidade: a definición social e territorial de Galicia na Alta Idade Media (seculos VIII e IX). Fundación Universitaria de Cultura, Santiago de Compostela
- Baliñas Pérez C (2002) De Covadonga a Compostela: Galicia en el marco de la construcción del Reino de Asturias. In: *La época de la Monarquía Asturiana: actas del simposio celebrado en Covadonga (8-10 de octubre de 2001)*. Real Instituto de Estudios Asturianos, Oviedo, pp. 367-390
- Brenk B (1987) Spolia from Constantine to Charlemagne: Aesthetics versus Ideology. *Dumbarton Oaks Papers* 41:103-109
- Brennan BJ (2003) Beta doses to spherical grains. *Radiat Meas* 3:299-303. [https://doi.org/10.1016/S1350-4487\(03\)00011-8](https://doi.org/10.1016/S1350-4487(03)00011-8)
- Brogio, GP (1988) *Archeologia dell'edilizia storica*. Edizioni New Press, Como.
- Caballero Zoreda L (1995) Método para el análisis estratigráfico de construcciones históricas o “lectura de paramentos”. *Informes de la Construcción* 453:37-46
- Caballero Zoreda L (1996) El análisis estratigráfico de construcciones históricas. In: Caballero Zoreda L, Escribano Velasco C (Eds.) (1996). *Arqueología de la Arquitectura*. El método arqueológico aplicado al proceso de estudio y de intervención en edificios históricos. Europa Artes Gráficas, Salamanca, pp. 55-74
- Caballero Zoreda, L (2004) Una experiencia en Arqueología de la Arquitectura. *Arqueología de la Arquitectura* 3:127-143.
- Cutler A (1999) Reuse or use? Theoretical and practical attitudes toward objects in the Early Middle Ages. In: *Ideologie e pratiche del reimpiego nell'alto Medioevo*. Atti delle settimane di Studio del Centro Italiano di Studi sull'Alto Medioevo, XLVI. CISAM, Spoleto: pp. 1055-1079
- Davies W (2007) *Acts of giving: individual, community, and church in tenth-century Christian Spain*. Oxford University Press, Oxford
- De Corte F, Vandenberghe D, Buylaert J-P, Van Den Haute P, Kucera J (2006) Relative and k_0 -standardized INAA to assess the internal (Th, U) radiation dose rate in the “quartz coarse-grain protocol” for OSL dating of sediments: Unexpected observations. *Nucl Instrum Meth A* 564:743-751 <https://doi.org/10.1016/j.nima.2006.04.009>
- Domingo Magaña JA (2009) La reutilización de material decorativo clásico durante la Tardoantigüedad y el altomedioevo en Cataluña. *Butlletí arqueològic* 32: 795-848
- Dunai TJ (2010) *Cosmogenic nuclides. Principles, concepts and applications in the Earth Surface Sciences*. Cambridge University Press, Cambridge.

- Dunne J, Elmore D, Muzikar P (1999) Scaling factors for the rates of production of cosmogenic nuclides shielding and attenuation at depth on sloped surfaces. *Geomorphology* 27:3-11 [https://doi.org/10.1016/S0169-555X\(98\)00086-5](https://doi.org/10.1016/S0169-555X(98)00086-5)
- Eaton T (2000) *Plundering the past. Roman stonework in Medieval Britain*. Tempus, Stroud
- Feathers JK, Johnson J, Kembel, SR (2008) Luminescence Dating of Monumental Stone Architecture at Chavín De Huántar, Perú. *J Archaeol Method Th* 15:266–296 <https://doi.org/10.1007/s10816-008-9053-9>
- Fernández-Suárez J, Arenas R, Abati J, Martínez Catalán JR, Whitehouse MJ, Jeffries TE (2007) U-Pb chronometry of polymetamorphic high-pressure granulites: An example from the allochthonous terranes of the NW Iberian Variscan belt. In Hatcher RD, Carlson MP, McBride JH, Martínez Catalán JR 4-D Framework of Continental Crust, The Geological Society of America, New York [https://doi.org/10.1130/2007.1200\(24\)](https://doi.org/10.1130/2007.1200(24))
- Freire Camaniel J (1998) *El monacato gallego en la Alta Edad Media*. Fundación Barrié, A Coruña
- Galbraith RF, Roberts RG, Laslett GM, Yoshida H, Olley H (1999) Optical dating of single and multiple grains of quartz from Jinmium Rock Shelter, Northern Australia: Part 1, Experimental design and statistical models. *Archaeometry* 41:339-364. <https://doi.org/10.1111/j.1475-4754.1999.tb00987.x>
- Goedicke C (2003) Dating historical calcite mortar by blue OSL: results from known age samples. *Radiat Meas* 37:409-15. [https://doi.org/10.1016/S1350-4487\(03\)00010-6](https://doi.org/10.1016/S1350-4487(03)00010-6)
- Goedicke C (2011) Dating mortar by optically stimulated luminescence: A feasibility study. *Geochronometria* 38:42-49. <https://doi.org/10.2478/s13386-011-0002-0>
- González Cuadra P (2007) *La Unidad de Corredoiras (Complejo de Órdenes, Galicia): Evolución estructural y metamórfica*. Serie Nova Terra, A Coruña
- Greenhalgh M (1989) *The survival of Roman Antiquities in the Middle Ages*. Duckworth, London
- Guerin G, Mercier N, Adamiec G (2011) Dose-rate conversion factors: update. *Ancient TL* 29: 5-8. [https://www.aber.ac.uk/temp-ancient-tl/issue16_2/adamiec_atl_16\(2\)_37-50.pdf](https://www.aber.ac.uk/temp-ancient-tl/issue16_2/adamiec_atl_16(2)_37-50.pdf)
- IGME (1981) *Mapa Geológico de España*. Magna 1:50.000. Hojas 46, 70 y 71
- Innes M (2000) *State and Society in the Early Middle Ages. The Middle Rhine Valley, 400-1000*. Cambridge University Press, Cambridge
- Isla Frez A (1992) *La sociedad gallega en la Alta Edad Media*. CSIC, Madrid
- Isla Frez A (1998) Aspectos de la organización del espacio en Galicia: El alto Tambre, siglos IX-XI. In: Barceló M, Toubert P, (eds.) "L'incastellamento". Actes des Rencontres de Gérone (26-27 Novembre 1992) et de Rome (5-7 Mai 1994), CSIC, Roma, pp. 57-70
- Krauskopf KB, Bird D (1995) *Introduction to geochemistry*. McGraw Hill, Columbus
- La Rocca C (2007) Le élites, chiese e sepolture familiari tra VIII e IX secolo in Italia settentrionale. In: Depreux P, Bougard F, Le Jan R, Les élites et leurs espaces. Mobilité, rayonnement, domination (du VIe au XIe siècle). Brepols, Turnhout, pp. 259-271
- Larrea JJ (2007) Construir iglesias, construir territorio: las dos fases altomedievales de San Román de Tobillas (Álava), in López Quiroga J (ed.), *Monasteria et Territoria. Elites, edilicia y territorio en el Mediterráneo medieval (siglos V-XI)*, Archaeopress, Oxford, pp. 321-336
- Liritzis I, Singhvi AK, Feathers JK, Wagner GA, Kadereit A, Zacharias N, Li SH, (2013) *Luminescence dating in archaeology, anthropology, and ge archaeology. An overview*. Springer, Heidelberg, Germany
- Loring García MI (1987) Nobleza e iglesias propias en la Cantabria altomedieval. *Studia histórica. Historia medieval* 5:89-121

Loscertales de Garcia de Valdeavellano P (1976) Tumbos del monasterio de Sobrado de los Monjes. Archivo Histórico Nacional, Madrid

Middendorf B, Hughes JJ, Callebaut K, Baronio G, Papayianni I (2005a) Investigative methods for the characterisation of historic mortars—Part 1: Mineralogical characterization. *Mater Struc* 38:761-769 <https://doi.org/10.1007/BF02479289>

Middendorf B, Hughes JJ, Callebaut K, Baronio G, Papayianni I (2005b) Investigative methods for the characterisation of historic mortars- Part 2: Chemical characterization. *Mater Struc* 38:771-780 <https://doi.org/10.1007/BF02479290>

Murray AS, Wintle AG (2000) Luminescence dating of quartz using an improved single-aliquot regenerative-dose protocol. *Radiat Meas* 32:57-73 [https://doi.org/10.1016/S1350-4487\(99\)00253-X](https://doi.org/10.1016/S1350-4487(99)00253-X)

Murray AS, Wintle AG (2003) The single aliquot regenerative dose protocol: Potential for improvements in reliability. *Radiat Meas* 37:377-381. [https://doi.org/10.1016/S1350-4487\(03\)00053-2](https://doi.org/10.1016/S1350-4487(03)00053-2)

Pallares Méndez MC (1979) El Monasterio de Sobrado: un ejemplo del protagonismo monástico en la Galicia medieval. Diputación de La Coruña, A Coruña

Portela Silva E (1995) Galicia y la monarquía leonesa. In: El reino de León en la Alta Edad Media VII. Centro de Estudios e Investigación "San Isidoro", León, pp. 12-70.

Portela Silva E (2002) Galicia y los reyes de Oviedo. In: La época de la Monarquía Asturiana: actas del simposio celebrado en Covadonga (8-10 de octubre de 2001). Real Instituto de Estudios Asturianos, Oviedo, pp. 351-365.

Prescott JR, Hutton JT (1994) Cosmic ray contributions to dose rates for luminescence and ESR dating: large depths and long term variations. *Radiat Meas* 23:497-500. [https://doi.org/10.1016/1350-4487\(94\)90086-8](https://doi.org/10.1016/1350-4487(94)90086-8)

Prudêncio MI, Dias MI, Gouveia MA, Marques R, Franco D & Trindade MJ (2009) Geochemical signatures of Roman amphorae produced in the Sado River estuary, Lusitania (Western Portugal). *Journal of Archaeological Science* 3:873-883

Quirós Castillo JA (1998) La sillería y las técnicas constructivas medievales: historia social y técnica de la producción arquitectónica. *Archeologia Medievale* XXV: 235-246

Quirós Castillo JA, Fernández Mier M (2012) Para una historia social de la arquitectura monumental altomedieval asturiana. In Caballero Zoreda L, Mateos Cruz P, García de Castro C (eds) *Asturias entre visigodos y mozárabes (Visigodos y Omeyas, VI - Madrid, 2010)*, CSIC, Madrid, pp. 27-53

Reimer PJ, Bard E, Bayliss A, Beck JW, Blackwell PG, Bronk Ramsey C, Grootes PM, Guilderson TP, Haflidason H, Hajdas I, Hattz C, Heaton TJ, Hoffmann DL, Hogg AG, Hughen KA, Kaiser KF, Kromer B, Manning SW, Niu M, Reimer RW, Richards DA, Scott EM, Southon JR, Staff RA, Turney CSM, Van Der Plicht J (2013) IntCal13 and Marine13 Radiocarbon Age Calibration Curves 0-50,000 Years cal BP. *Radiocarbon* 55:1869-1887. https://doi.org/10.2458/azu_js_rc.55.16947

Sánchez-Pardo JC (2015) Power strategies in the early medieval churches of Galicia (711-910 AD), In Sánchez-Pardo JC, Shapland M. (eds.) *Churches and Social Power in Early Medieval Europe (ca. 400-1100 AD)*. Integrating archaeological and historical approaches. Brepols, Turnhout, pp. 227-268

Sánchez-Pardo JC, Blanco-Rotea R (2014) Early Medieval Churches. History, Archeology and Heritage (2013-2017). Marie Curie EMCHAHE project. *The European Archaeologist* 42:83-85

Sánchez-Pardo JC, Blanco-Rotea R, Sanjurjo-Sánchez J (2017a) The church of Santa Comba de Bande and early medieval Iberian architecture: new chronological results. *Antiquity* 357:1011-1026, doi: <https://doi.org/10.15184/aqy.2017.83>

- Sánchez-Pardo JC, Blanco-Rotea R, Sanjurjo-Sánchez J (2017b) Tres arquitecturas altomedievales orensanas: Santa Eufemia de Ambía, San Xés de Francelos y San Martiño de Pazó. *Arqueología de la Arquitectura* 14: e062, doi: <http://dx.doi.org/10.3989/arq.arqt.2017.017>
- Sanjurjo-Sánchez J (2016) Dating historical buildings: an update on the possibilities of absolute dating methods. *Int J Archit Herit* 10:620-635. <https://doi.org/10.1080/15583058.2015.1055384>
- Sanjurjo-Sánchez J, Gomez-Heras M, Fort R, Alvarez de Buergo M, Izquierdo Benito R, Angel Bru M (2016) Dating fires and estimating the temperature attained on stone surfaces. The case of Ciudad de Vascos (Spain). *Microchem J* 127:247-255. <https://doi.org/10.1016/j.microc.2016.03.017>
- Sánchez Zufiaurre L (2007) Técnicas constructivas medievales. Nuevos documentos arqueológicos para el estudio de la Alta Edad Media en Álava. Universidad del País Vasco, Bilbao
- Soraluce Blond JR, Fernández Fernández J (2001) Arquitecturas de la provincia da Coruña, Vol. XVI. Deputación Provincial da Coruña, A Coruña
- Stella, G, Fontana D, Gueli AM, Troja SO (2013) Historical mortars dating from OSL signals of fine grain fraction enriched in quartz. *Geochronometria* 40:153-164. <https://doi.org/10.2478/s13386-013-0107-8>
- Urbanova P, Guibert, P (2017) Methodological study on single grain OSL dating of mortars: Comparison of five reference archaeological sites. *Geochronometria*, 44:77-97. <https://doi.org/10.1515/geochr-2015-0050>
- Urbanova P, Hourcade D, Ney C, Guibert P (2015) Sources of uncertainties in OSL dating of archaeological mortars: The case study of the Roman amphitheatre “Palais-Gallien” in Bordeaux. *Radiat Meas* 72: 100-110. <https://doi.org/10.1016/j.radmeas.2014.11.014>
- Utrero MA, Sastre I (2012) Reutilizando materiales en las construcciones de los siglos VII-X. ¿Una posibilidad o una necesidad?. *Anales de Historia del Arte* 22 (II): 309-323
- Vandenbergh D, De Corte F, Buylaert JP, Kucera J, Van Den Haute P, (2008) On the internal radioactivity in quartz. *Radiat Meas* 43:771-775. <https://doi.org/10.1016/j.radmeas.2008.01.016>
- VVAA (2013) Enciclopedia del Románico en Galicia: A Coruña. Fundación Santa María la Real, Aguilar de Campoo
- Ward-Perkins B (1999) Re-using the Architectural Legacy of the Past, *entre idéologie et pragmatism*. In: Brogiolo GP, Ward-Perkins B. (Eds.) *The idea and ideal of town between Late Antiquity and the Early Middle Ages*. Brill, Leiden, pp. 225-244.
- Wood S (2006) *The proprietary church in the medieval West*. Oxford University Press, Oxford

CAPTIONS

Fig. 1 Location of San Martiño de Armental church in NW Iberia

Fig. 2 View of the church from the North

Fig. 3 View of the church from the NE. Below: plan of the church adapted from Soraluce and Fernández (2001: 260)

Fig. 4 Reused material in Phase II: inverted epigraph with the date 871 AD and upper part of a twin window. Places in which mortar samples were taken are also indicated

Fig. 5 Photogrammetric model of the epigraph discovered in the church, with and without texture and different digital illuminations in order to obtain a better reading of the inscription “Era DCCCC et VIII A(nnos)”. Model made with AgiSoft Photoscan Pro software

Fig. 6 Photogrammetric model of the North and South façades of the church. Model made with AgiSoft Photoscan Pro software

Fig. 7 Stratigraphic Units (UEs) differentiated over the ortoimages of the façades north and south and over pictures of east and west façades

Fig. 8 Harris Matrix of the construction sequence of the church of San Martiño de Armental

Fig. 9 View of the North exterior wall of the church with Phase I (UE009) remarked and indications of the places in which mortar samples were taken.

Fig. 10 Up: romanesque phase in the south façade of the building, with reused ashlar around the door and the window. The upper part of the wall was refurbished in Modern or Contemporary times, as it can also be seen in the interior of the church (image below)

Fig. 11 Other churches with reused stones close to San Martiño de Armental: Santiago de Prógalo (Lugo), Santa María de Uriz (Castroverde), San Lourenzo de Carelle (Sobrado) and San Pedro de Vilanova (Palas de Rei)

Fig. 12 Example of a XRD plot of the mortar sample ARM-08 that shows quartz, anortite and muscovite as major mineral components

Fig. 13 Normalized REE patterns of the studied mortars and the ceramic sample. It can be observed that the pattern of samples ARM-01 and ARM-03 completely fit and also samples ARM-08 and ARM-09 (ceramic) fit with a shift observed in the ARM-08 sample

Fig. 14 Plots of distribution equivalent doses of aliquots obtained for OSL of mortar samples. The first column show histograms, the second one the Kernel Density plot and the third one the Radial Plots obtained. Samples: A: ARM-01; B: ARM-02; C: ARM-03; D: ARM-08

Fig. 15 Geological situation of the church (represented by a yellow square). Taken from Fernández-Suarez et al. 2007

Fig. 16 Aerial view of the church of San Martiño de Armental and the nearest gneiss outcrops (red spots)

Fig. 17 Petrological analysis of the 5 samples: a) Crenulated foliation in gneiss in M-1 (magnifier, 8 mm); b) Gneiss (magnifier, 8 mm) in M-2; c) M-3: Quartz in mosaic texture and biotite (thin section); d) Biotite and chlorite in kink texture in M-3 (thin section); e) M-4: Quartz (grey) and feldspars (white) in magnifier (8 mm); f) M-5 Quartz, feldspars and micas (thin section)

Figure 18 Chronotipology of the different construction techniques employed in San Martiño de Armental